TID (forecasting) models - MSTIDs

M. Sivakandan
Leibniz Institute of Atmospheric Physics (IAP) at the University of Rostock
Kühlungsborn
Germany.

2nd PITHIA NRF Training School supported by T-FORS project, February 8, 2024, Leuven

Outline

- Models for MSTIDs
  - GAIA (Ground to top of the Atmosphere Ionosphere coupled model)
  - MICO (**M**idlatitude **I**onosphere electrodynamics **CO**upling model)
  - SAMI3 (Sami3 is Another Model of the Ionosphere)
- MSTIDs climatology and probabilistic forecasting
- MSTIDs climatological model
- Summary

Methodology

GPS

- ✓ To obtain perturbation component of TEC, which could be caused by MSTID, 1-hour running average of TEC was subtracted from the original TEC time series for each pair of satellites and receivers, and converted the slant to vertical TEC.
- ✓ MSTID activity defined as ΔTEC/TEC, where ΔTEC is the standard deviation of the perturbation component within 1 hour, and TEC is 1-hour average absolute vertical TEC.

GAIA

- ✓ GAIA is an atmosphere ionosphere Coupled model that covers the whole atmospheric regions from the ground surface to the upper thermosphere/ionosphere.
- ✓ In the upper atmosphere, horizontal and vertical resolution of the GAIA data is 1°×1° latitude, longitude and 10 km respectively. Temporal resolution 10 minutes.
- ✓ Detrended TEC obtained by subtracting 2-hour running average from the TEC, and calculated standard deviation of the detrended TEC in 2 hours. MSTID activity was obtained as a ratio of the standard deviation to the 2-hour averaged TEC.

Global TEC perturbation in GAIA: A case study

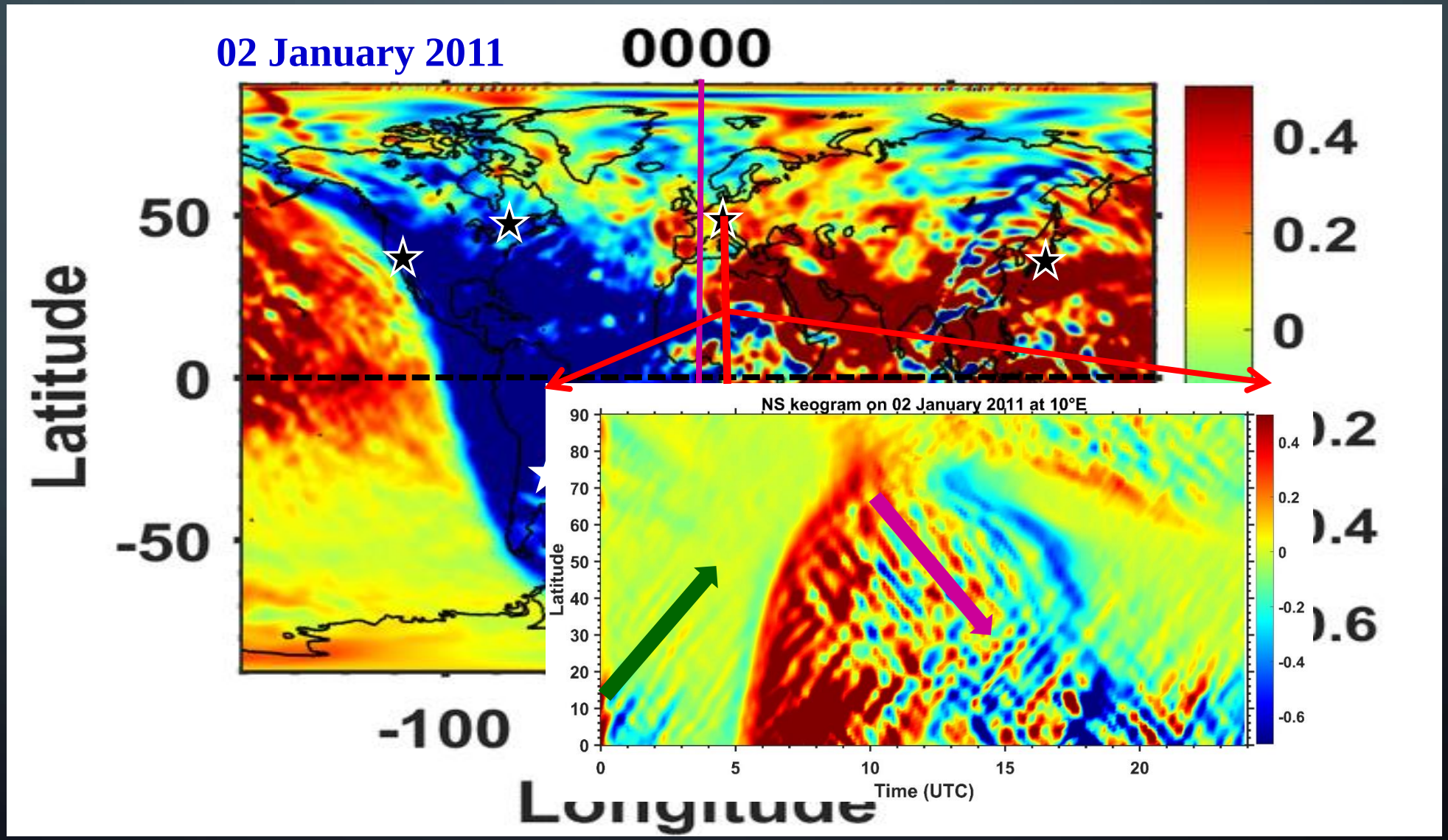

Location of the study

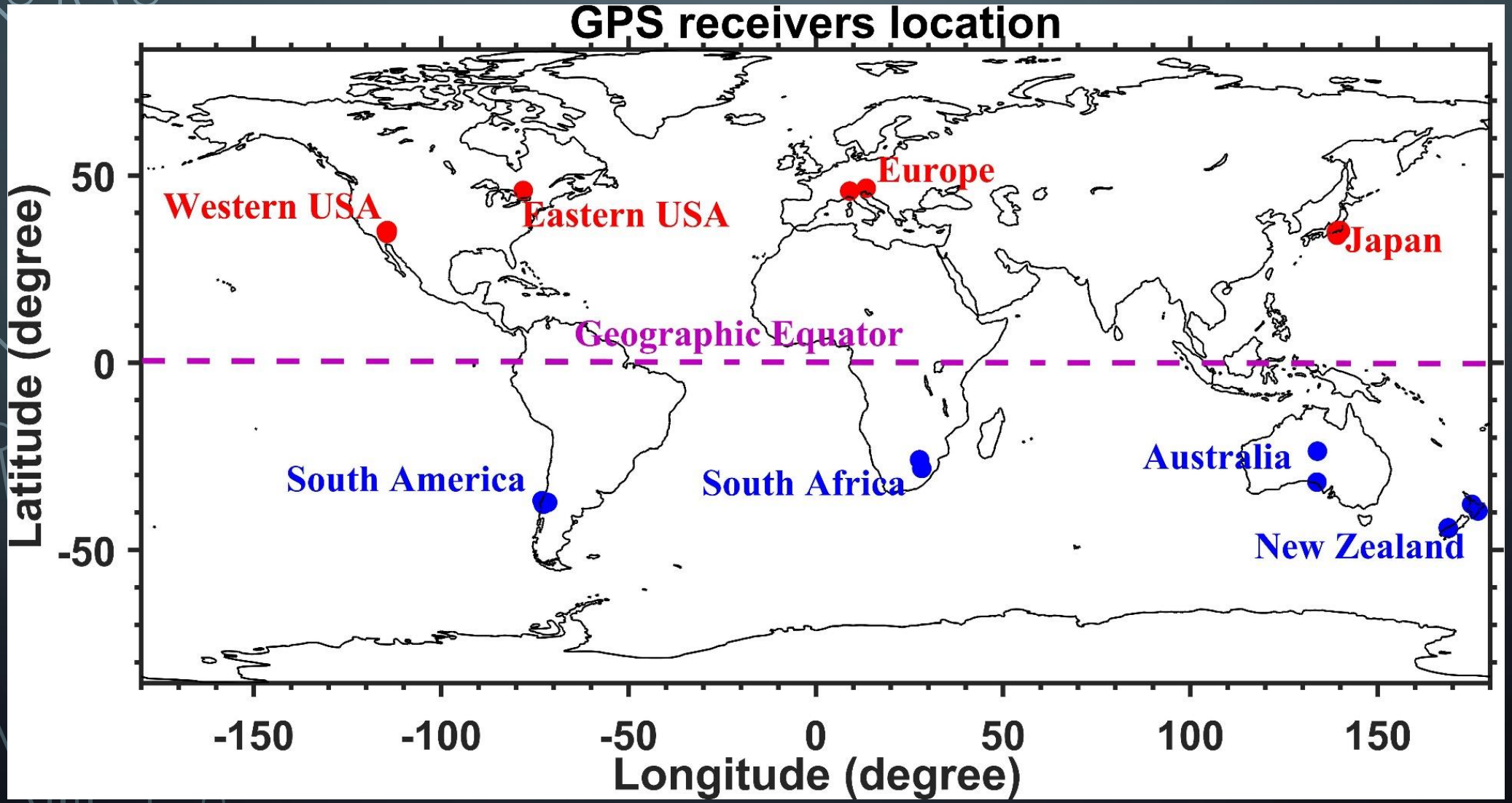

What causes the daytime MSTIDs in GAIA?

Wind variance derivation method

- Zonal, meridional and mean wind variance are calculated using GAIA data during the year 2011 as follows:

$$\overline{u'^2} = \overline{(u - \bar{u})^2}$$

$$\overline{v'^2} = \overline{(v - \bar{v})^2}$$

$$\overline{U'^2} = \overline{u'^2} + \overline{v'^2}$$

u ⇢ zonal wind

$\bar{u}$ ⇢ 2 hour averaged zonal wind

$\overline{u'^2}$ ⇢ average of zonal wind variance

v ⇢ meridional wind

$\bar{v}$ ⇢ 2 hour averaged meridional wind

$\overline{v'^2}$ ⇢ average of meridional wind variance

$\overline{U'^2}$ ⇢ mean wind variance

However, here we used only the meridional wind variance for the comparison purpose

Seasonal and temporal variation in Southern Hemisphere

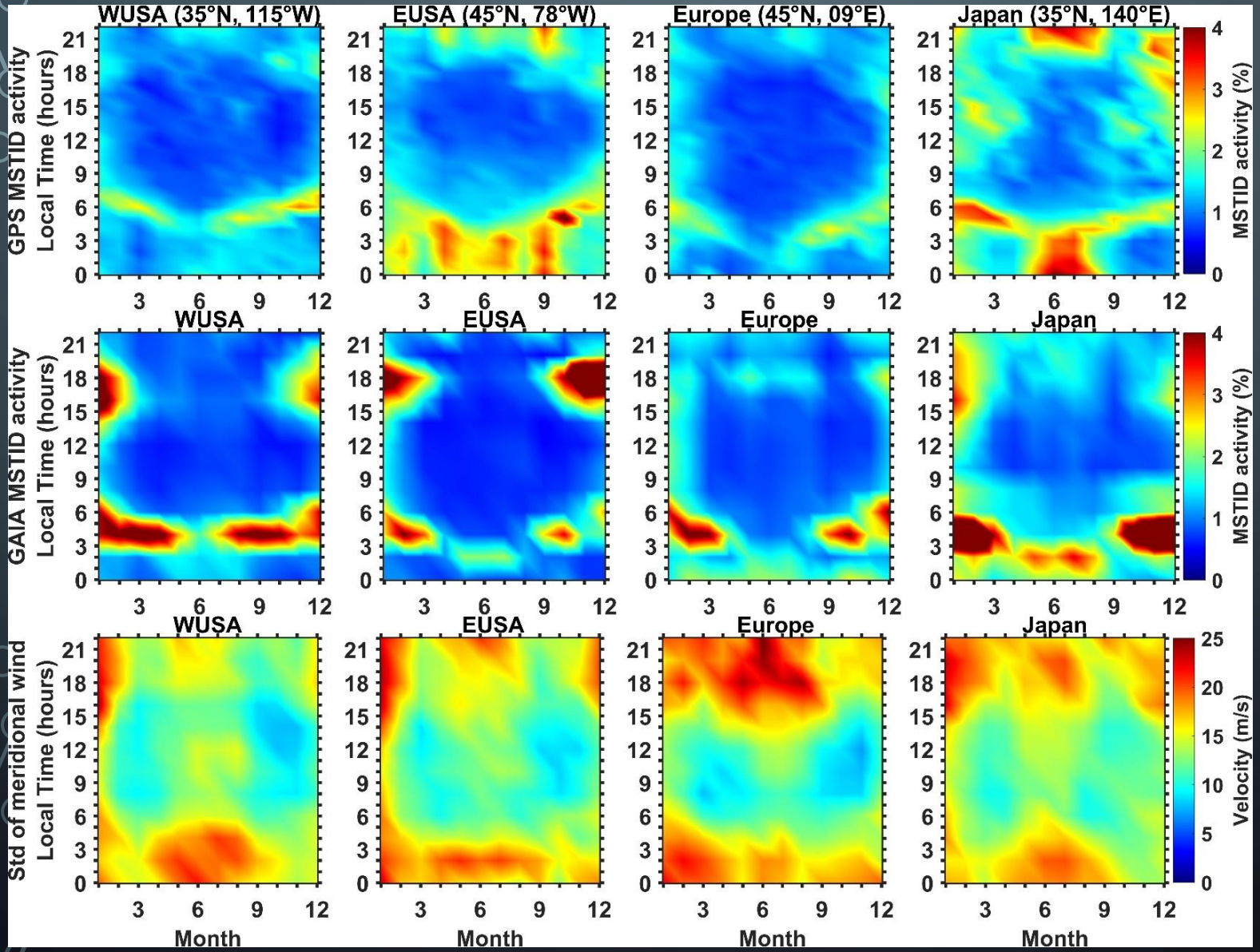

Daytime mean MSTID activity and wind variance in NH

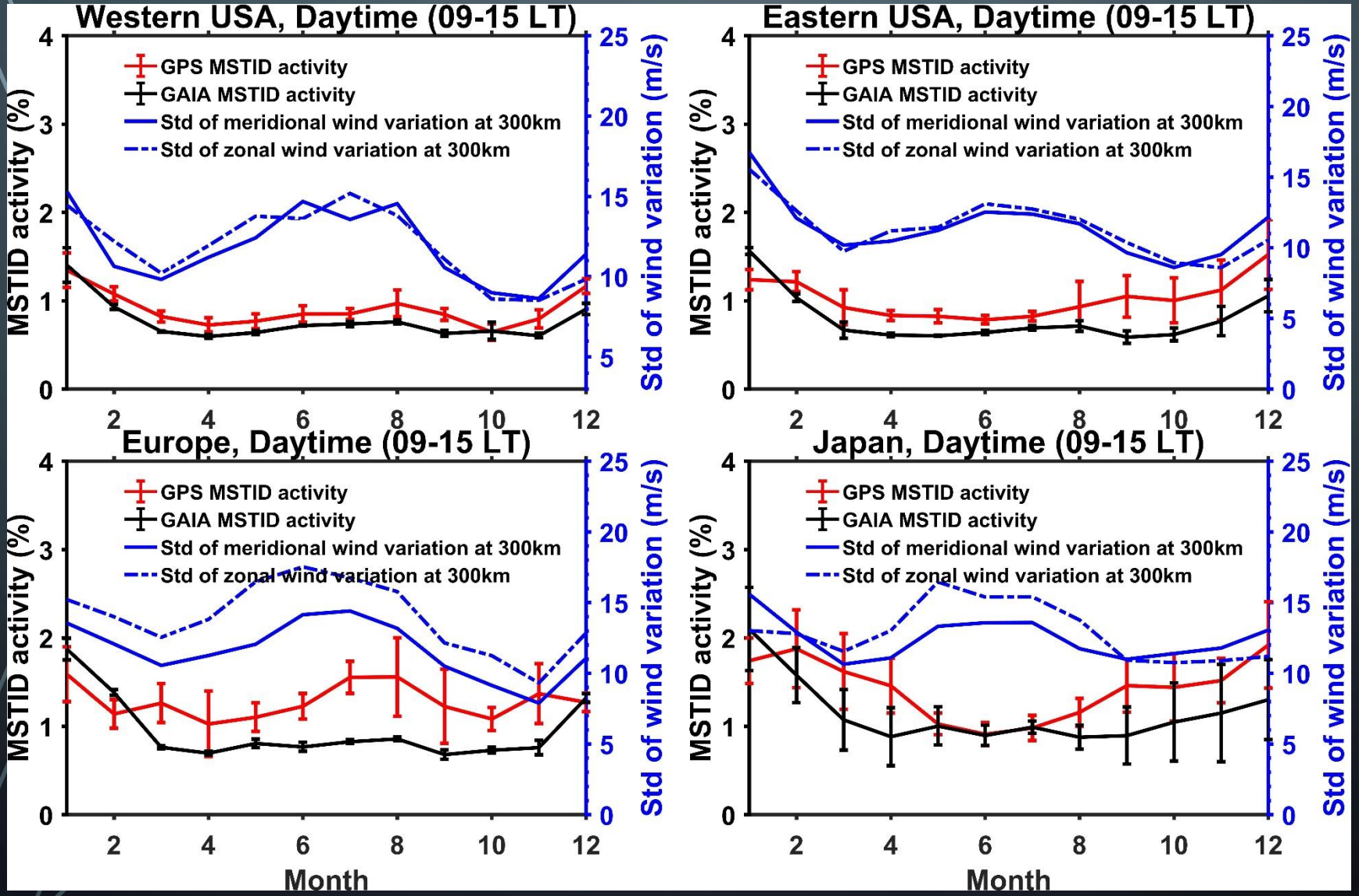

Seasonal and temporal variation in Southern Hemisphere

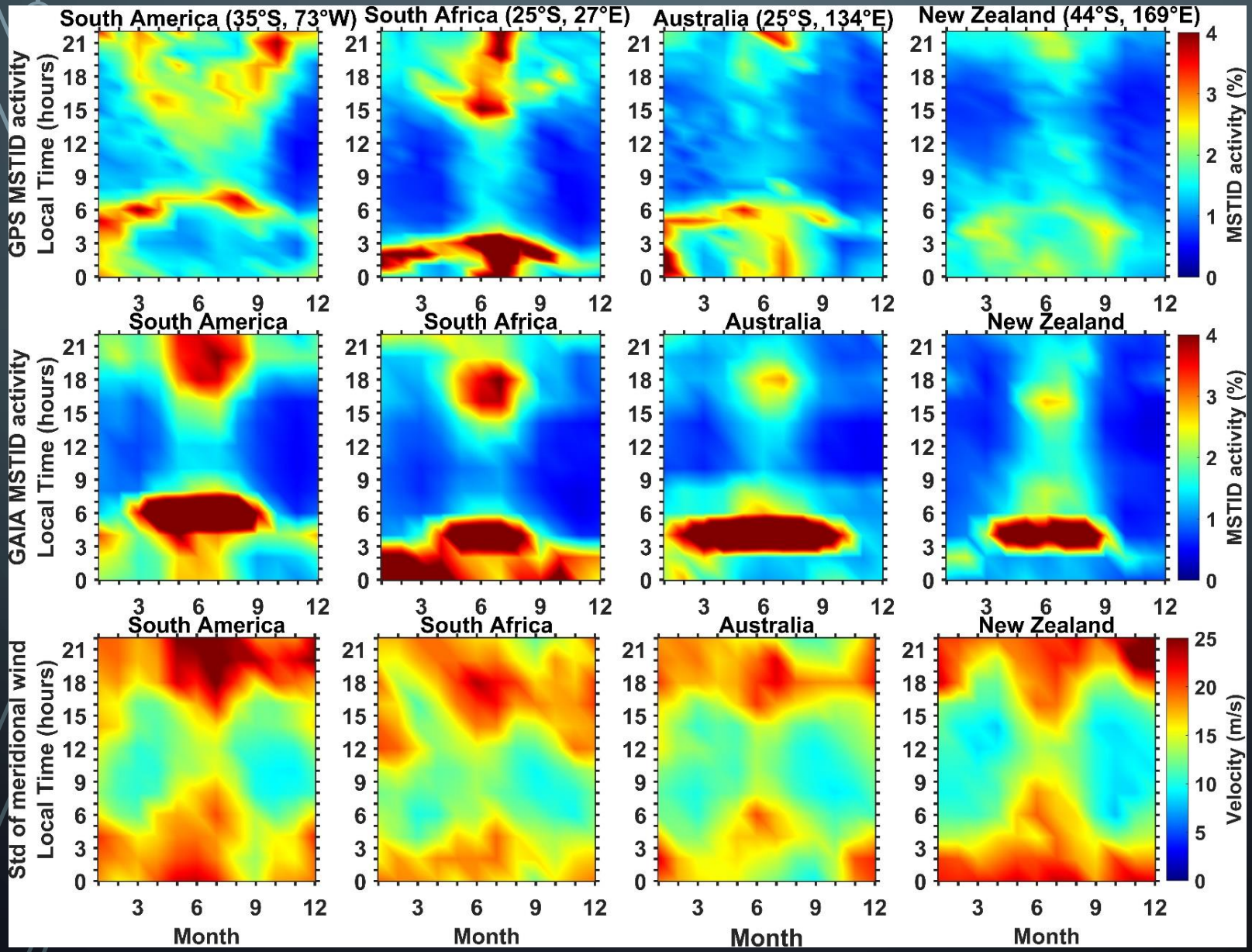

Daytime mean MSTID activity and wind variance in SH

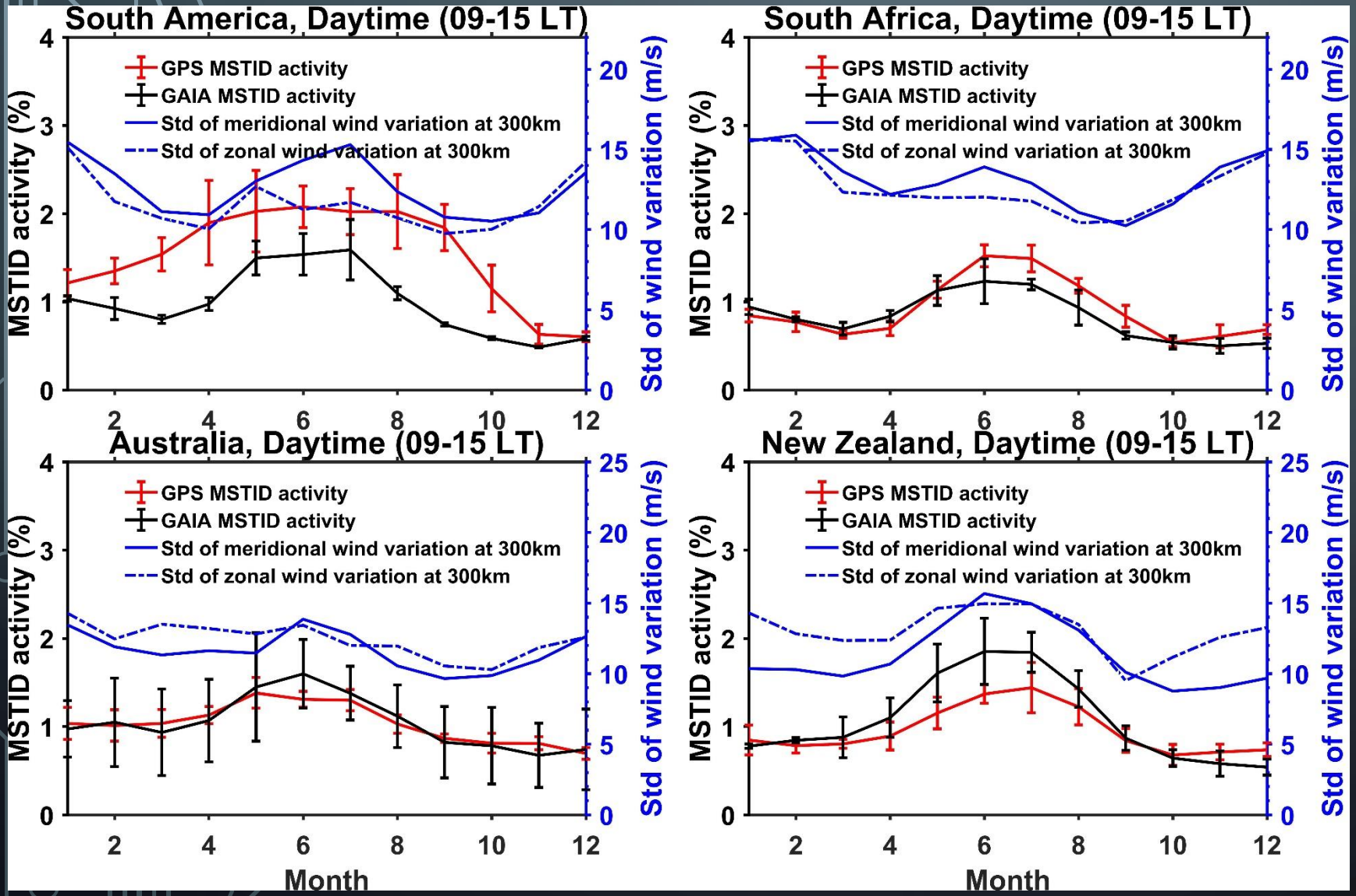

- ✓ The winter peak in amplitude of the meridional wind variations coincide with the winter peak in the daytime MSTID activity. This is because GWs with ***large amplitude are responsible for MSTIDs in winter.***

Longitudinal variation of MSTID activity in GPS and GAIA

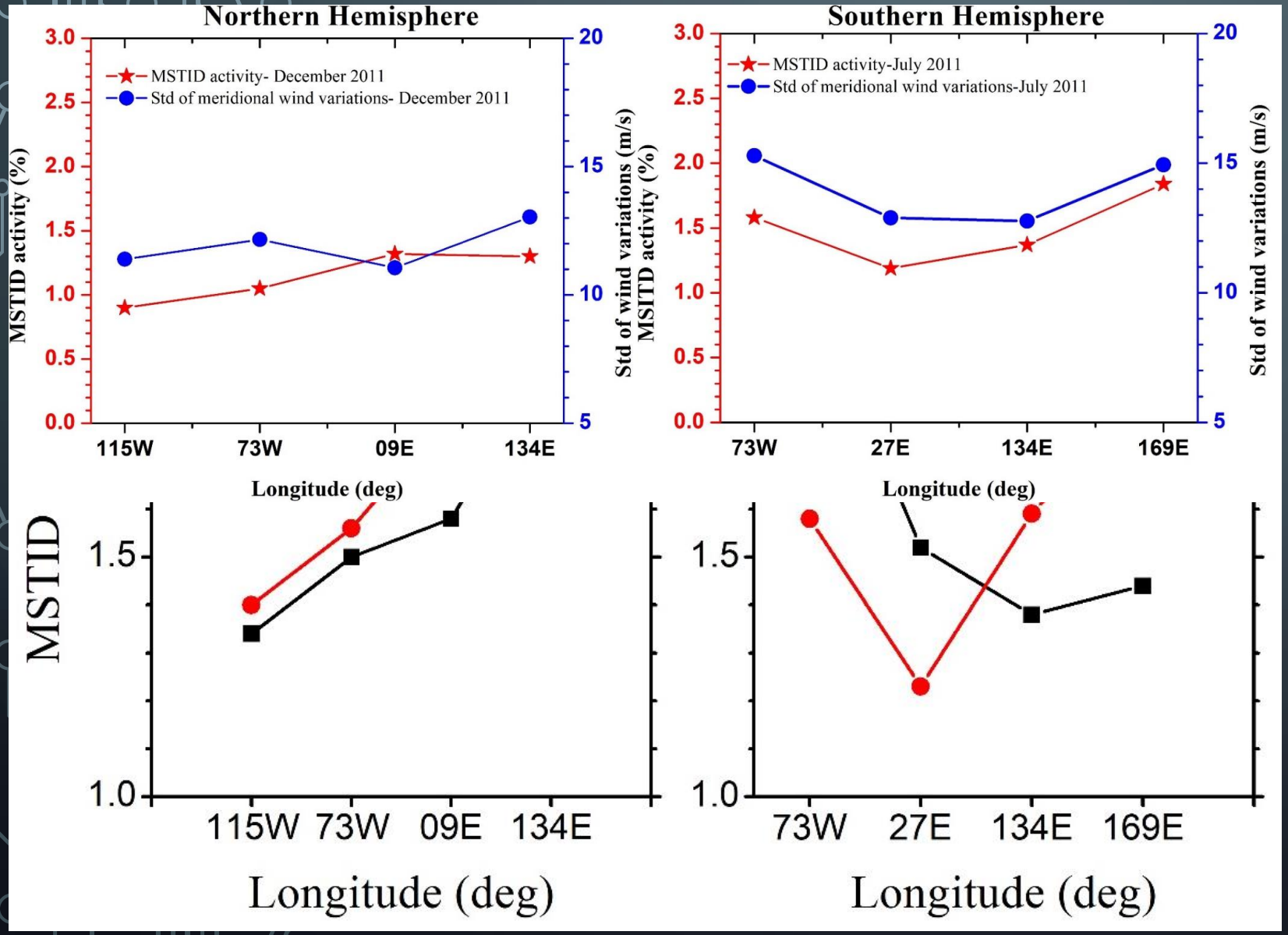

- ✓ In the northern hemisphere, daytime MSTID activities are high over the Japanese sector than the US sector
- ✓ In the southern hemisphere, daytime MSTID activities are high over the Pacific Ocean sector than the African sector
- ✓ ***GAIA can successfully reproduce the longitudinal variation of day time MSTID activity***

What causes the seasonal discrepancy between wind and MSTIDs activity?

A typical day in summer

Over South Africa

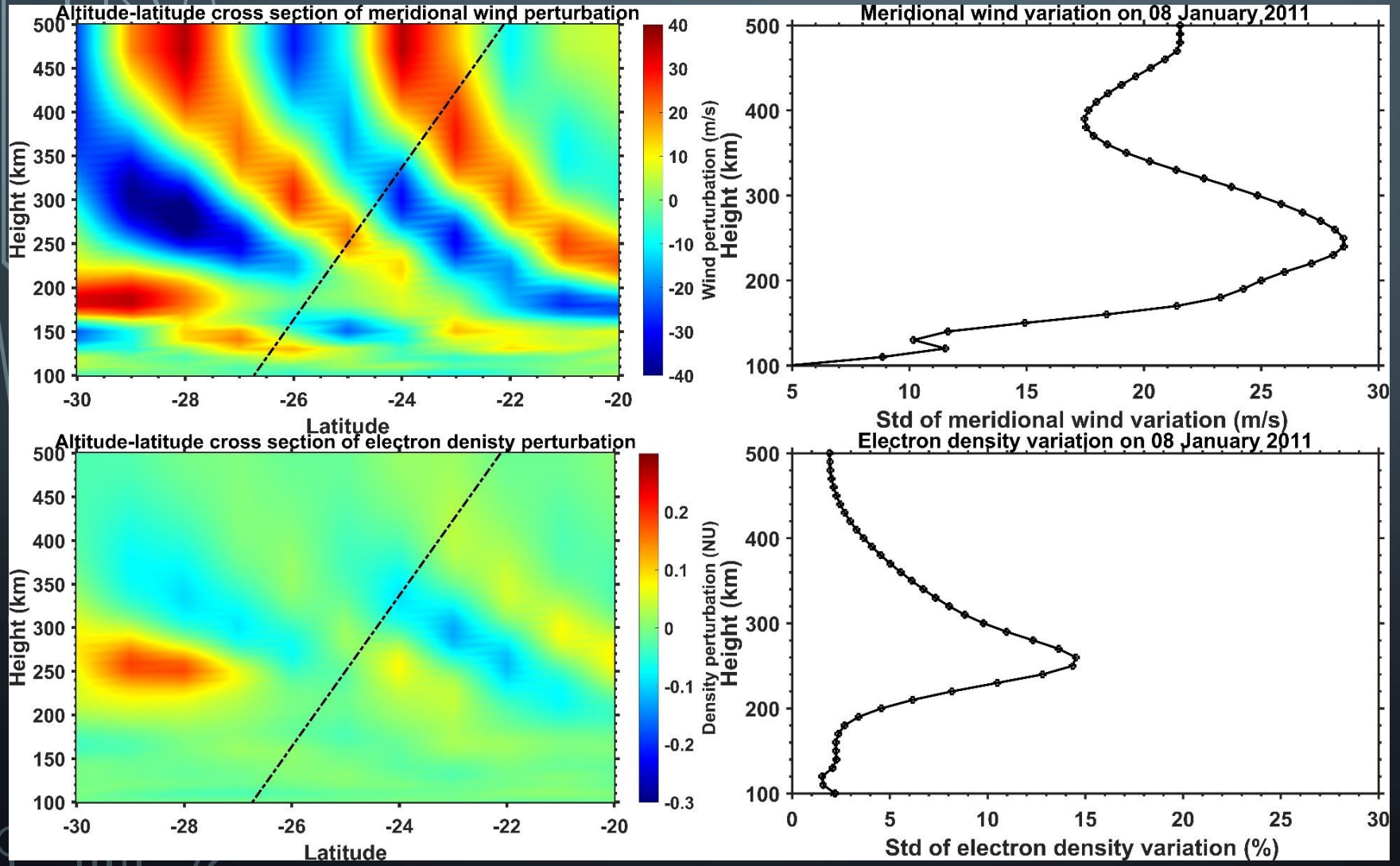

- ✓ The GWs propagate poleward in summer.
- ✓ The ion perturbation velocity smaller for the poleward propagating GWs.

What causes the seasonal discrepancy between wind and MSTIDs activity?

A typical day in winter

Over South Africa

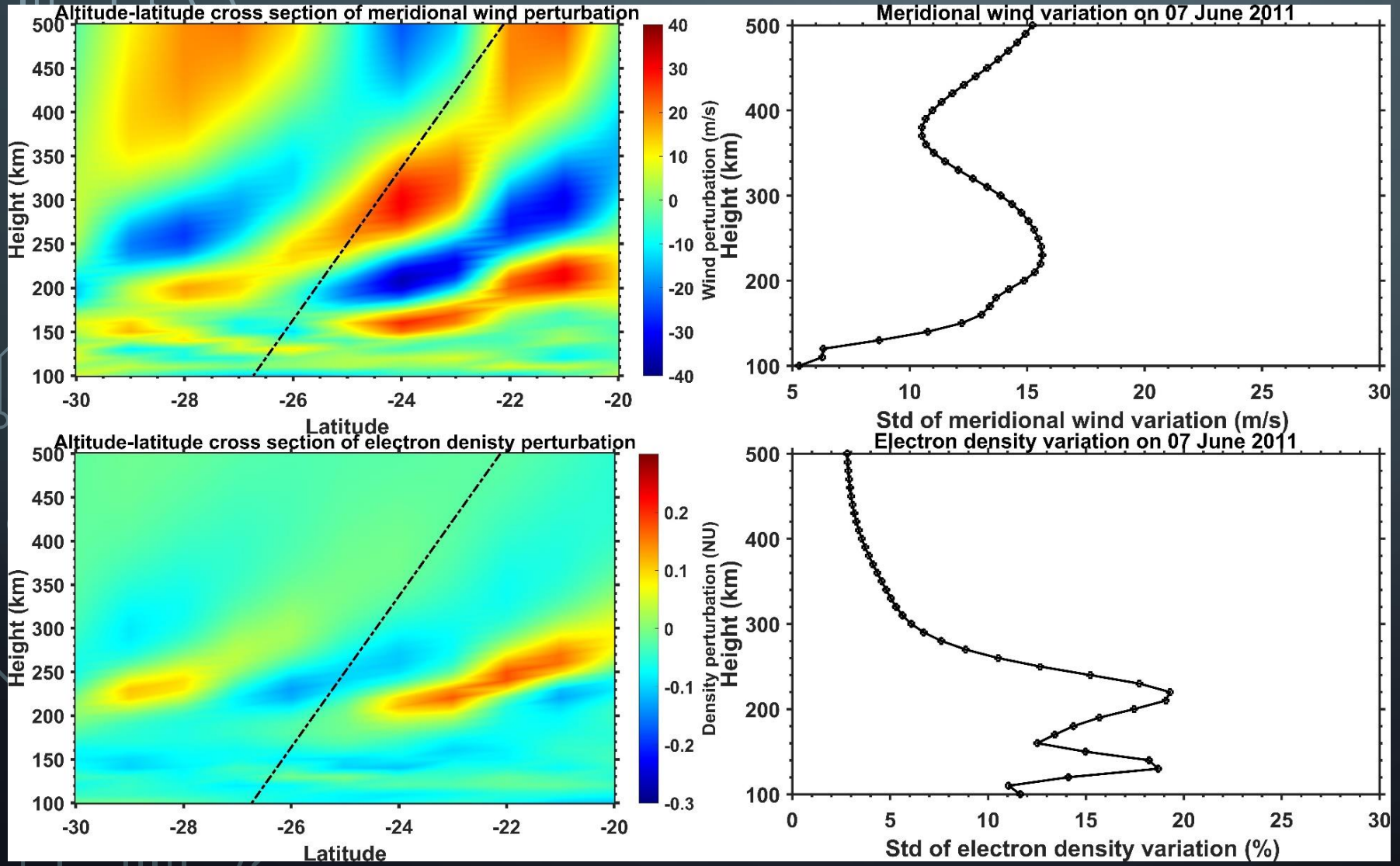

- ✓ The GAIA simulation show that GWs propagate toward equator in winter.
- ✓ The ion perturbation velocity is larger for the equatorward propagating GWs than that for the poleward propagating GWs.
- ✓ Therefore, the ***propagation direction of the GW is responsible for the largest MSTID activity in winter.***

Sivakandan et al. (2021)

MICO model

The fundamental plasma physics of MIECO is based on the previous model developed by Yokoyama et al. (2009), which is a three dimensional model with fixed dip angle.

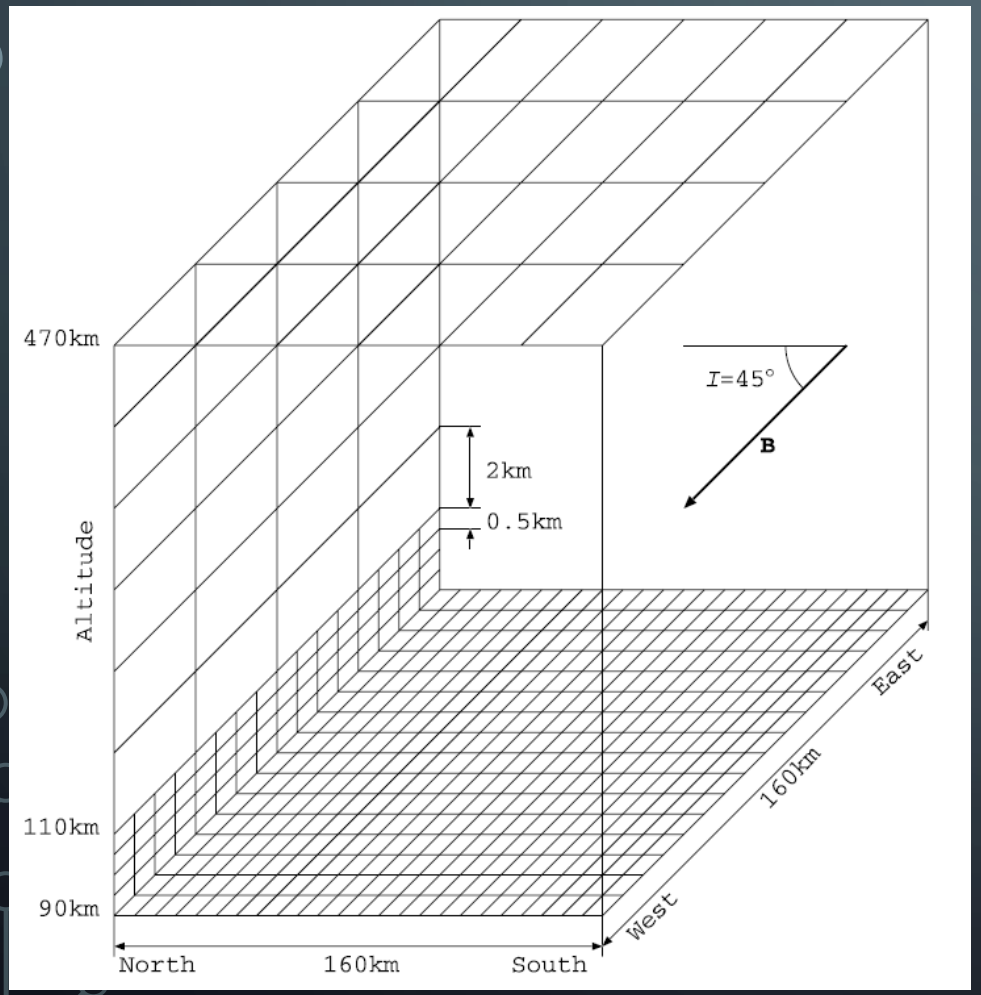

Yokoyama et al. (2009)

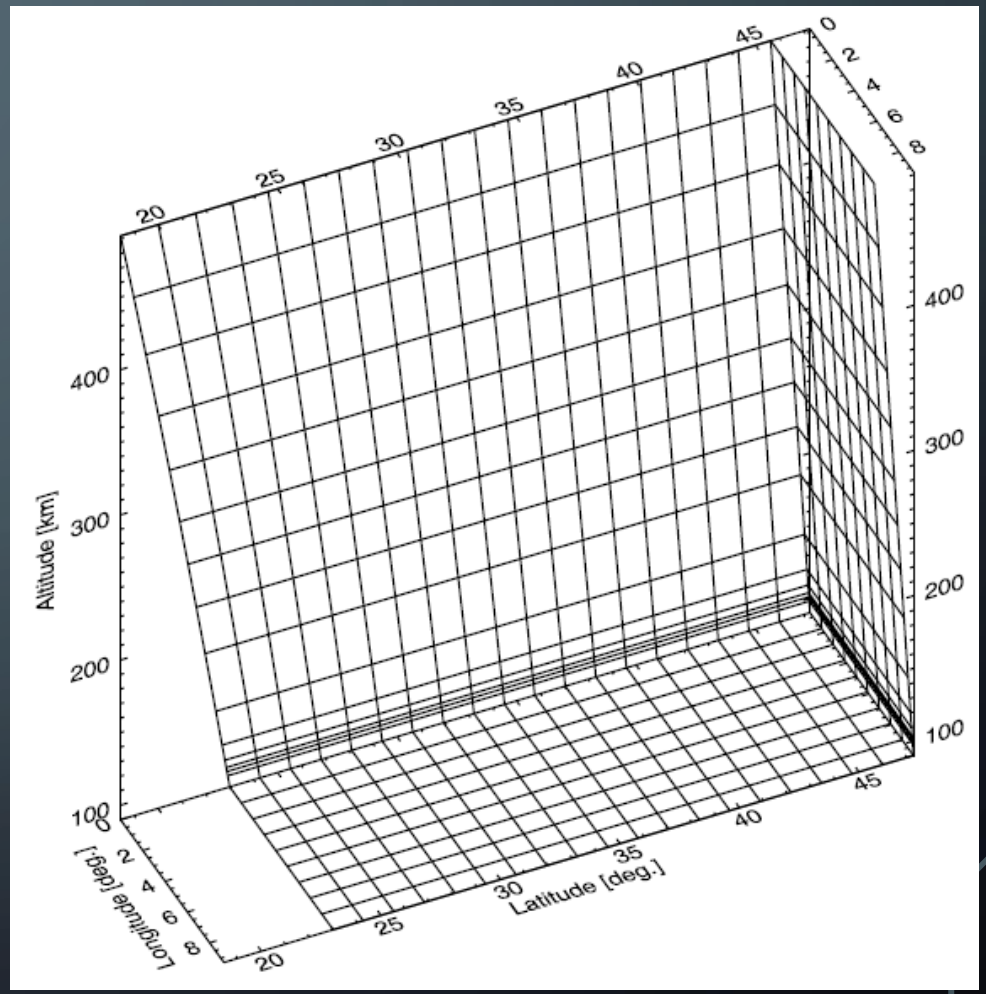

Yokoyama and Hysell. (2010)

Continued…,

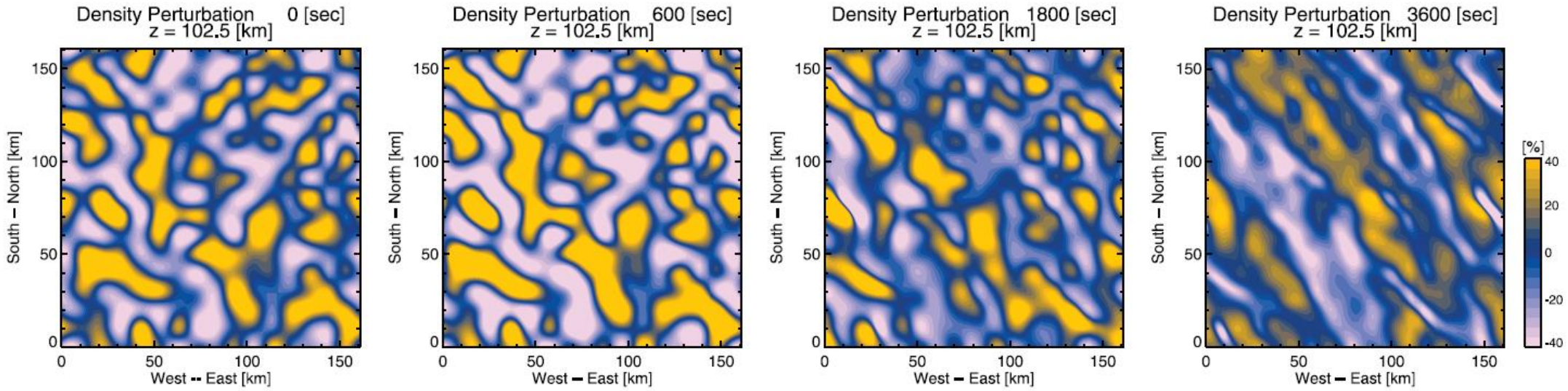

1. The Es-layer instability plays a major role in seeding NW-SE structure in the F region, and the Perkins instability is required to amplify its perturbation;

2. The rotational wind shear in the E region produces southwestward phase propagation of the NW-SE structure in both the E and F regions; and

3. The coupling process has a significant effect on the scale of the Es-layer perturbation rather than the growth rate of the Es-layer instability.

Yokoyama et al. (2009)

Continued…,

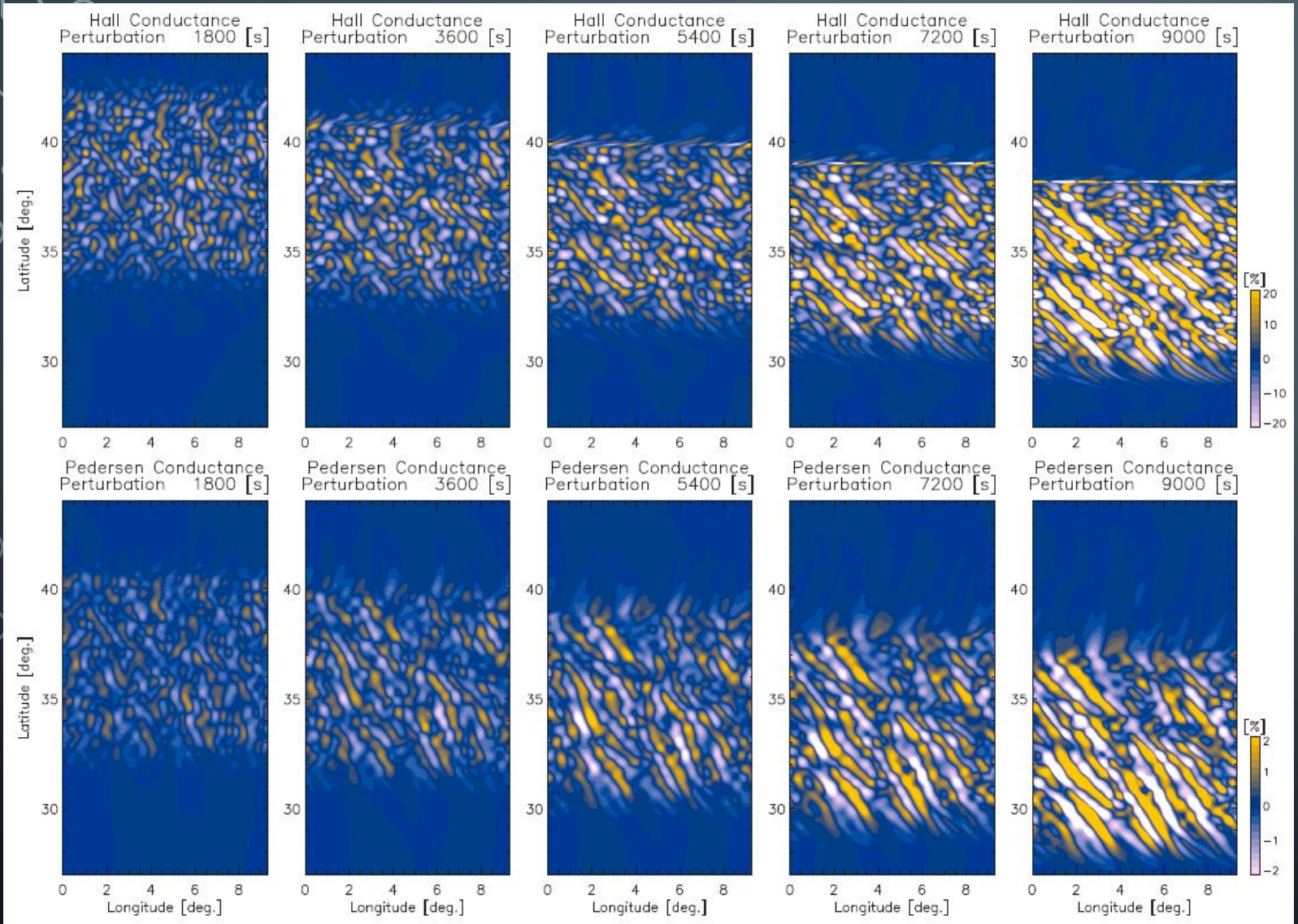

- ✓ The polarization process in the E region driven by neutral winds is essentially important for the full development of MSTIDs as well as the seeding of NW–SE perturbation in the F region.
- ✓ Both sporadic *E* (*Es*) layer and Perkins instabilities have the scale dependence that a shorter wavelength mode tends to stop growing within a shorter period, whereas a very long wavelength mode grows so slowly in the *E* region that it does not effectively seed the Perkins instability in the *F* region. As a result, the typical wavelength of MSTIDs (100–200 km) can be spontaneously generated without scale-dependent forcing.

Yokoyama and Hysell. (2010)

Yokoyama (2013)

SAMI3 model

- SAMI3 models the coupled, dynamical evolution of the fundamental, physics based equations relating to Earth's upper atmosphere
- SAMI3 uses a dipole coordinate system, which is advantageous to break down the governing equations that describe the physics parallel and perpendicular to the magnetic field line
- SAMI3 has its origins in a two-dimensional model named SAMI2 (Huba et al., 2008).
- The SAMI2 model solves the ion and momentum equations for seven ion species (H+, He+, N+, O+, N2+, NO+, and O2+) in a longitudinal slice of the ionosphere for altitudes ranging from approximately 100 km to over 1000 km. A dipole coordinate system is use for the grid spacing with one direction along the field line.
- SAMI3 is similar to SAMI2, except it includes grid spacing in the longitudinal direction and a potential solver, in effect modeling the ionosphere on a global scale.
- In the original SAMI2 code, the electric field is calculated from a climatological, analytical, or data-driven model. However, SAMI3 solves for the potential self-consistently within the model.

Duly ,Ph.D. Thesis, (2014)

Continued…,

In SAMI2/3, the conversion from geographic to dipole (q, p,) coordinates is a three-step process and includes the following conversions:

Spherical Geographic → Spherical Titled → Spherical Eccentric → Dipole

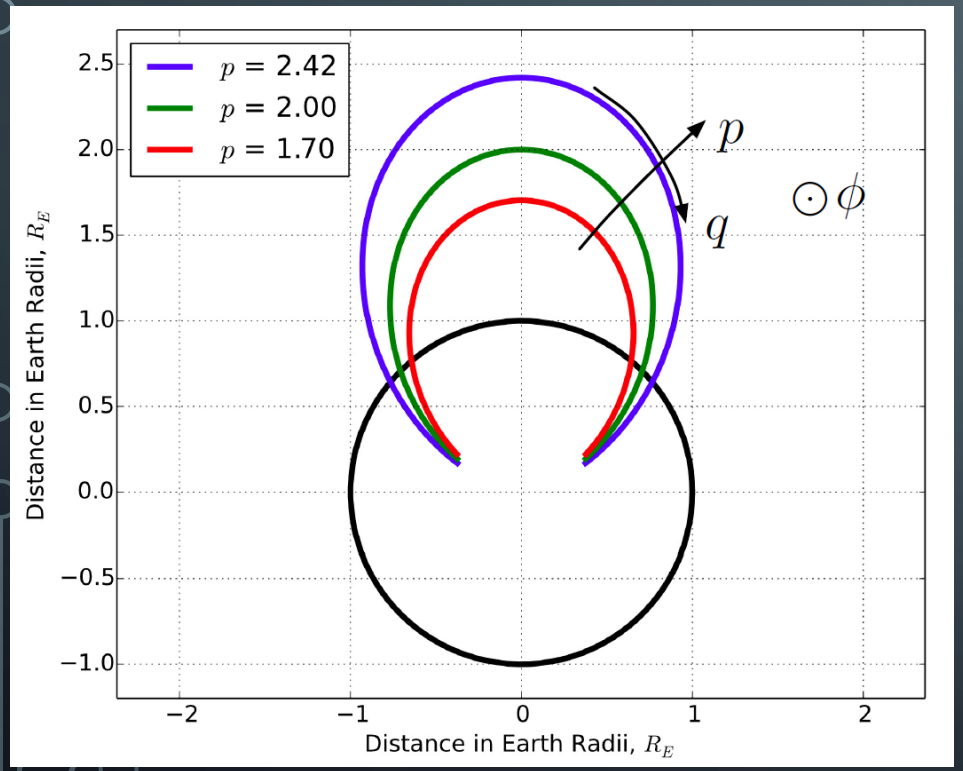

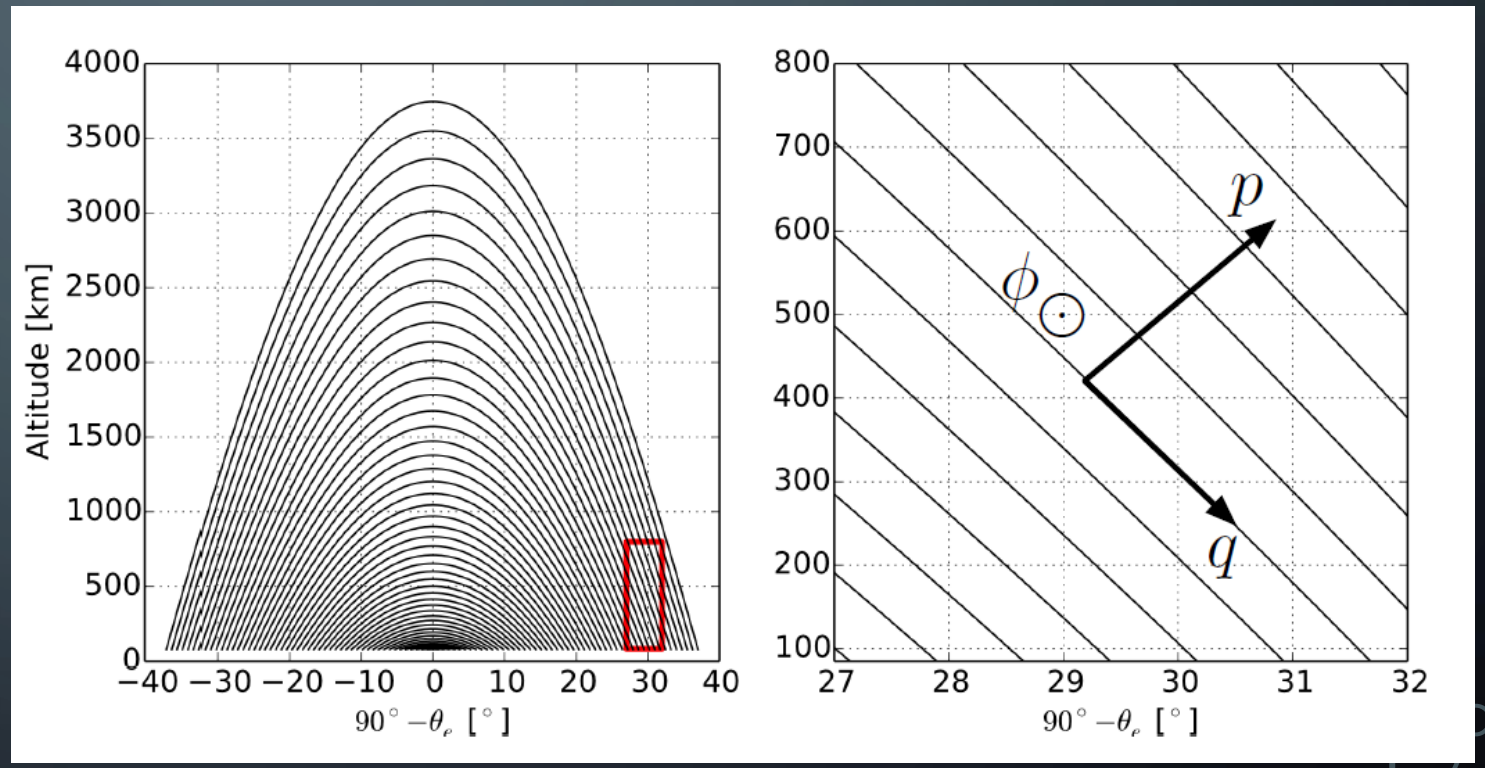

Duly ,Ph.D. Thesis, (2014)

Continued…,

Quantity	Description	Value for γ Calculation	Source
H_n	Neutral scale height	40 km	*Perkins* (1973)
k_x	Perturbation wave vector	$0.04038\ \mathrm{km}^{-1}$	Case 2 input perturbation
k_y	Perturbation wave vector	$0.04813\ \mathrm{km}^{-1}$	Case 2 input perturbation
U_x	Neutral wind	-43.85 m/s	SAMI3 / HWM93
U_y	Neutral wind	131.55 m/s	SAMI3 / HWM93
U_z	Neutral wind	-40.92 m/s	SAMI3 / HWM93
E_x	Electric field	-1.48 mV/m	SAMI3 (Equation 5.13)
E_y	Electric field	9.71×10^{-3} mV/m	SAMI3 (Equation 5.13)
B	Magnetic field strength	2.86×10^{-5} T	SAMI3
D	Magnetic dip angle	$46.72°$	SAMI3

Duly ,Ph.D. Thesis, (2014)

Case 1: random perturbation

$$\Delta\Sigma_{\mathrm{P}} = \frac{\Sigma_{\mathrm{P,\,pert}} - \Sigma_{\mathrm{P,\,control}}}{\Sigma_{\mathrm{P,\,control}}} \times 100\ [\%].$$

$\Delta\Sigma_p$ ⟶ The parameter represent the MSTIDs dynamics

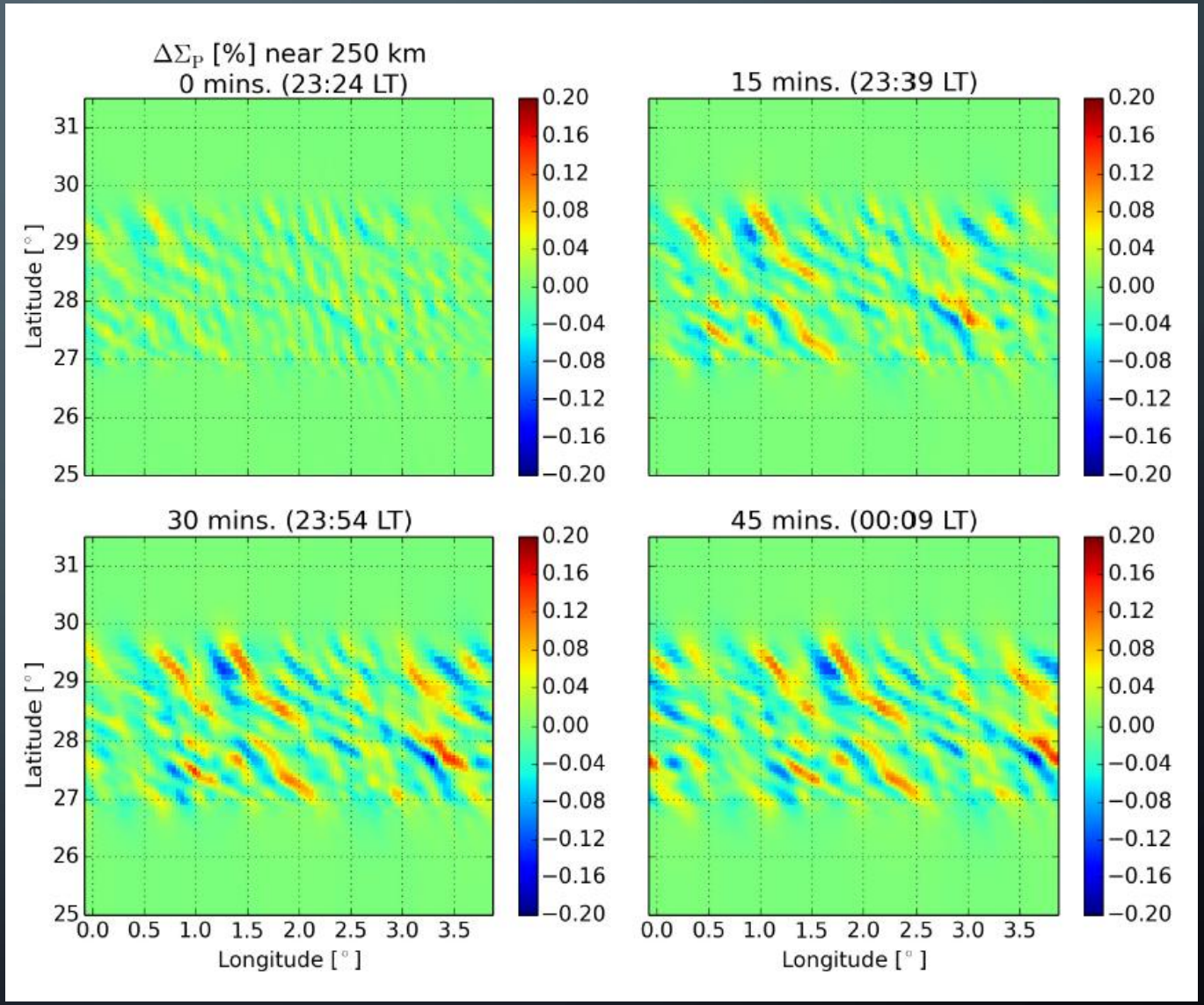

Duly ,Ph.D. Thesis, (2014)

Case 2: Specified wave perturbation

The redistribution of ne is prescribed by a wave having = 100 km at an angle = 40° with respect to magnetic east at 250-km altitude in the Northern Hemisphere. The amplitude of the perturbation is approximately 30 km in the magnetic field line direction

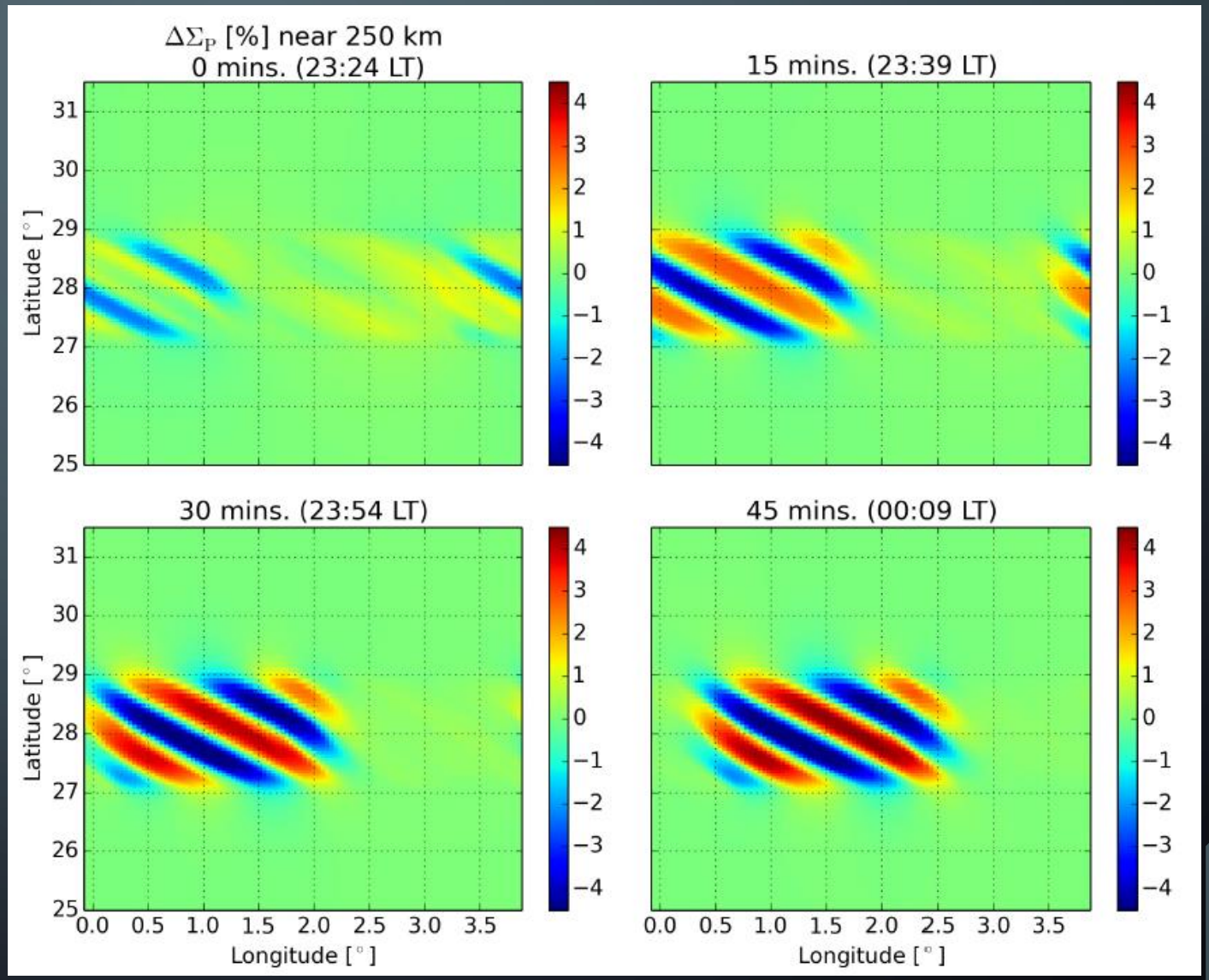

Duly ,Ph.D. Thesis, (2014)

Growth rate of MSTIDs in SAMI3 simulation

- ✓ The growth of the MSTID in SAMI3 is larger than the linear theory for the first 30 minutes, at which point the values saturate in the model.
- ✓ Differences between these values may be the result of the neutral wind influence from the conjugate hemisphere
- ✓ This simulation could not reproduce the southwest propagation of the MSTIDs

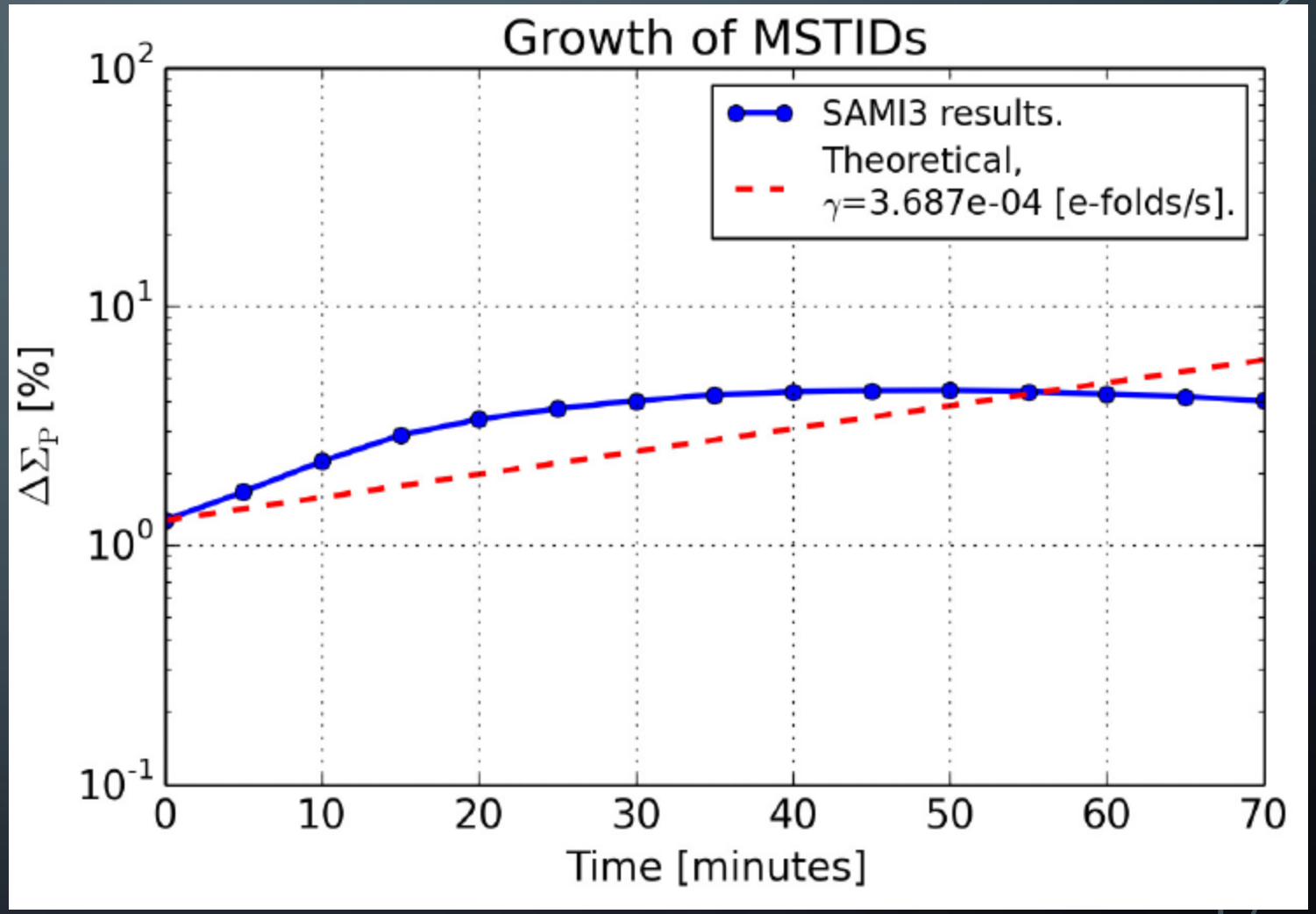

Duly ,Ph.D. Thesis, (2014)

WP3:MSTIDs climatology and probabilistic forecasting

M. Sivakandan[1], J. Mielich[1], J.L.Chau[1], D. Burešová[2], D. Kouba[2] V. Barta[3], K. A. Berényi[3], K. Koutroumbas [4], A. Belehaki[4] D. Altadill[5], T. Seggarra[5], and T. Verhulst[6]

1. Leibniz-Institute of Atmospheric Physics, Schloßstraße 6, 18225 Kühlungsborn, Germany
2. Institute of Atmospheric Physics, Czech Academy of Sciences, Prague, Czech Republic
3. Institute of Earth Physics and Space Science, Csatkai E. u. 6-8, 9400 Sopron, Hungary
4. National Observatory of Athens, IAASARS, Vas. Paylou & I. Metaxa, Athens, Greece
5. Observatori de l'Ebre, CSIC – Universitat Ramon Llull, C.\ Observatori, 3-A, 43520 Roquetes, Spain
6. Royal Meteorological Institute of Belgium & Solar Terrestrial Centre of Excellence, Brussels, Belgium

WP3: GENERAL APPROACH

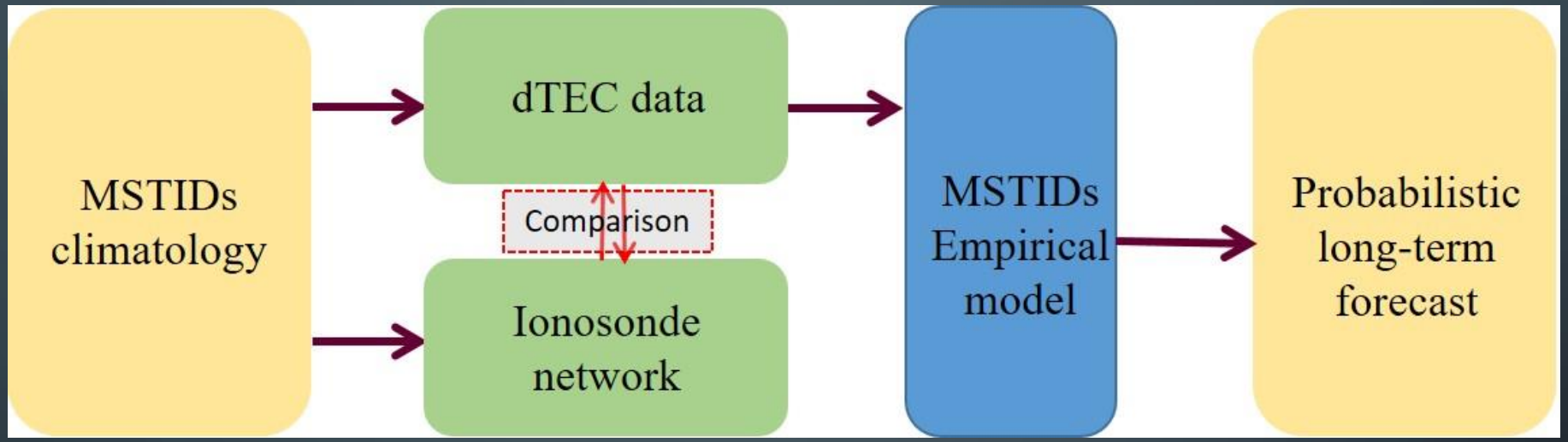

The schematic diagram presents the general approach which will be followed in WP3.

METHODOLOGY: MSTID CLIMATOLOGY

Methodology: detrended total electron content (dTEC)

- ✓ To obtain perturbation component of TEC, which could be caused by MSTIDs, 1-hour running average of TEC was subtracted from the original TEC time series for each pair of satellites and receivers, and converted the slant to vertical TEC.
- ✓ Temporal resolution is 30 seconds, and the spatial resolution is 0.25×0.25 latitude and longitude.

02 December 2020 at 13:00 UT

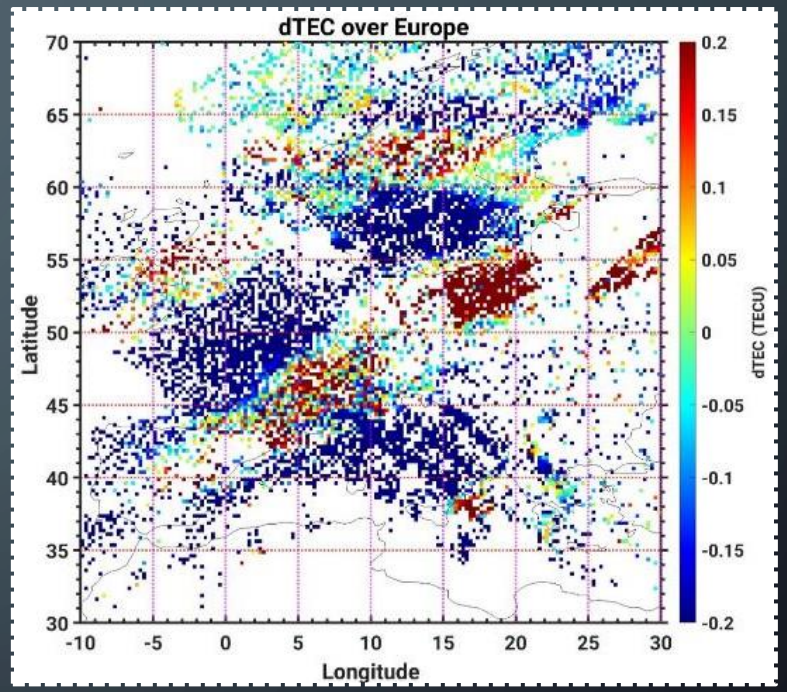

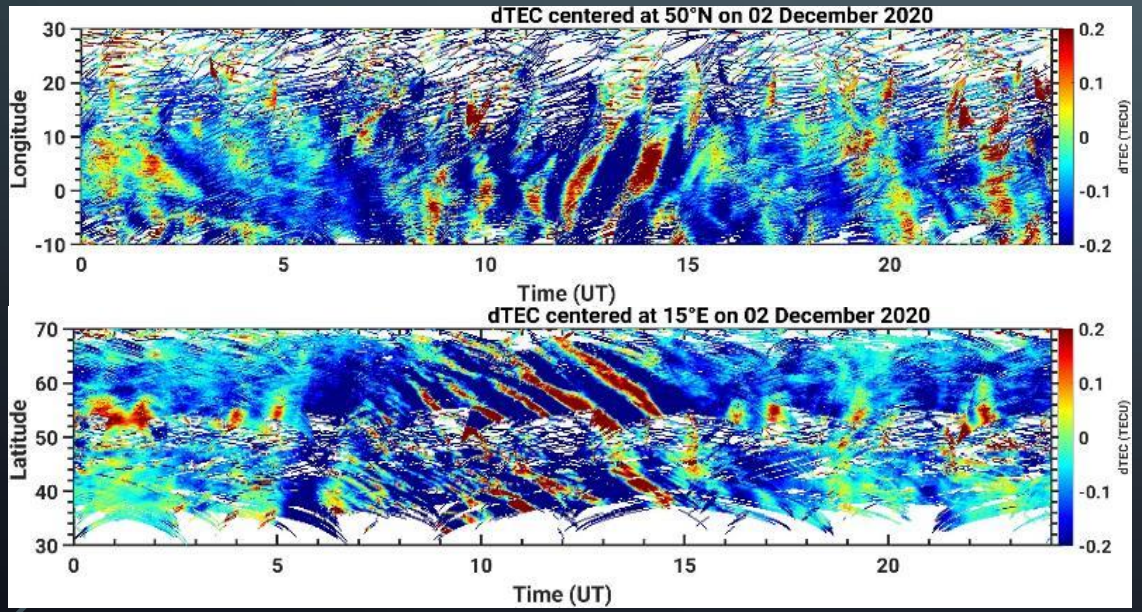

- ✓ Keogram analysis is used to identify the propagation direction, wavelength and phase speed of the MSTIDs

Sivakandan et al. WP3

METHODOLOGY: MSTID CLIMATOLOGY

Label	Direction	Characteristics of phase front in EW and NS keogram
1	North	EWK-aligned; NSK-progression towards north
2	East	EWK-progression towards east; NSK-aligned
3	South	EWK-aligned; NSK-progression towards south
4	West	EWK-progression towards west; NSK-aligned
5	Northeast	EWK-progression towards east; NSK-progression towards north
6	Southeast	EWK-progression towards east; NSK-progression towards south
7	Southwest	EWK-progression towards west; NSK-progression towards south
8	Northwest	EWK-progression towards west; NSK-progression towards north

We analyzed data for the four seasons i.e. two equinoxes (March and September) and two solstices (June and December) of three years (2014, 2016, 2020)

METHODOLOGY: MSTID CLIMATOLOGY

Methodology: ionograms

URSI-code	Name	Latitude	Longitude	Ionosonde type
JR055	Juliusruh	54.60	13.40	DPS-4D
FF051	Fairford	51.70	358.50	DPS-4D
RL052	Chilton	51.50	359.40	DPS-1
DB049	Dourbes	50.10	4.60	DPS-4D
PQ052	Pruhonice	50.00	14.60	DPS-4D
SO148	Sopron	47.63	16.72	DPS-4D
RO041	Rome	41.90	12.50	DPS-4
EB040	Roquetes	40.80	0.50	DPS-4D
VT139	San Vito	40.60	17.80	DPS-4D
AT138	Athens	38.00	23.50	DPS-4D
EA036	El Arenosillo	37.10	353.30	DPS-4D
NI135	Nicosia	35.03	33.16	DPS-4D

METHODOLOGY: MSTID CLIMATOLOGY

Methodology: ionograms

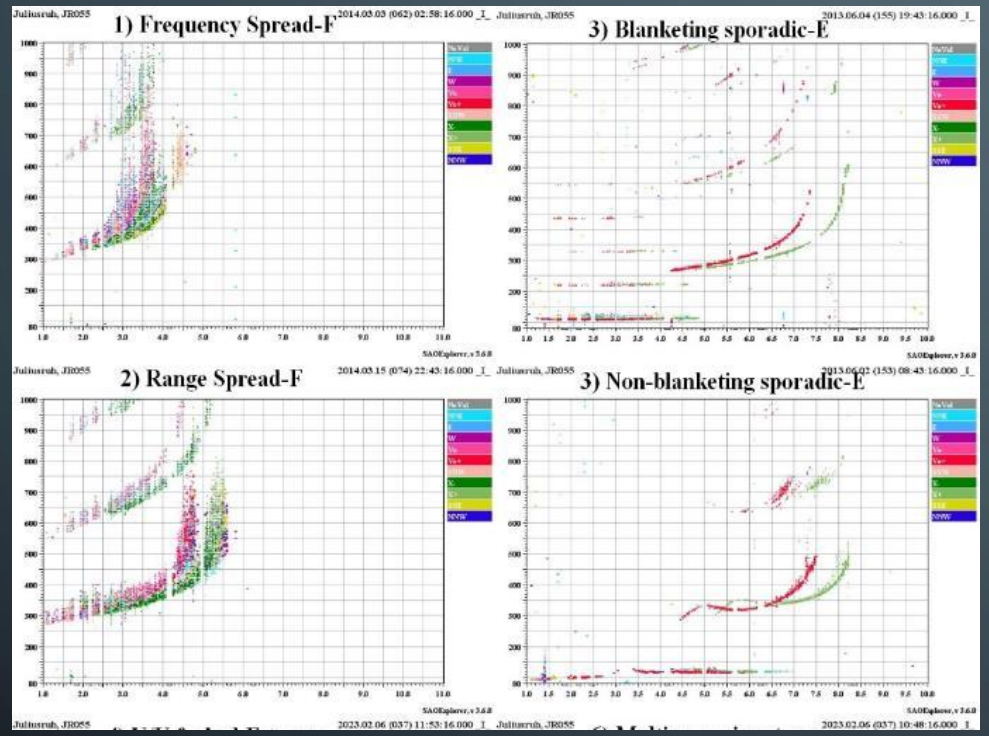

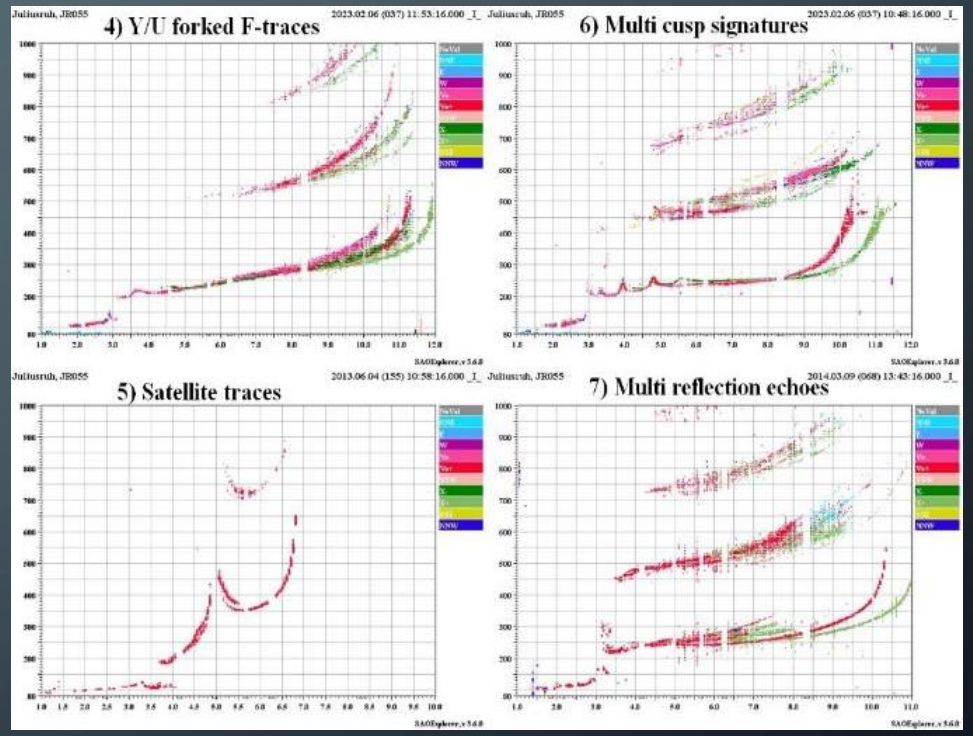

- We analyzed data for the four seasons i.e. two equinoxes (March and September) and two solstices (June and December) of three years (2014, 2016, 2020).
- Only hourly ionograms are considered for the analysis: in total 24*366=8784 ionograms per station

RESULTS: MSTID CLIMATOLOGY

MSTID occurrence climatology using dTEC

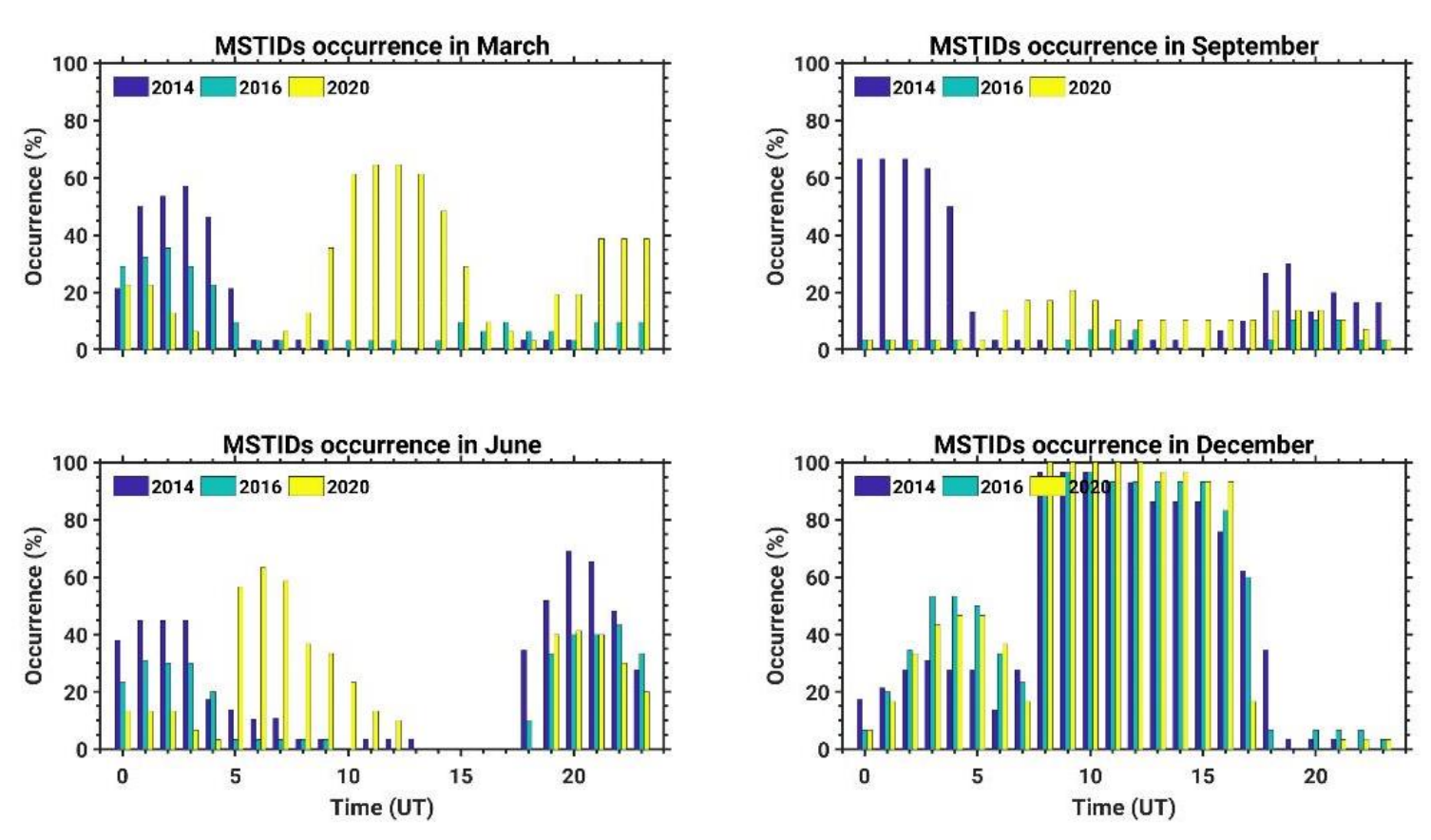

- Daytime MSTID occurrence is more during December than any other months
- Pre-midnight MSTID occurrence is high in June
- Post-midnight MSTID occurrence is high in equinoxial months
- Anomalous day and nighttime MSTID occurrence are noted in the months of March and June and that is higher in 2020 than other years.
- Significant number of early morning MSTID occurrence are noted in solstice months

RESULTS: MSTID CLIMATOLOGY

MSTID propagation climatology using dTEC

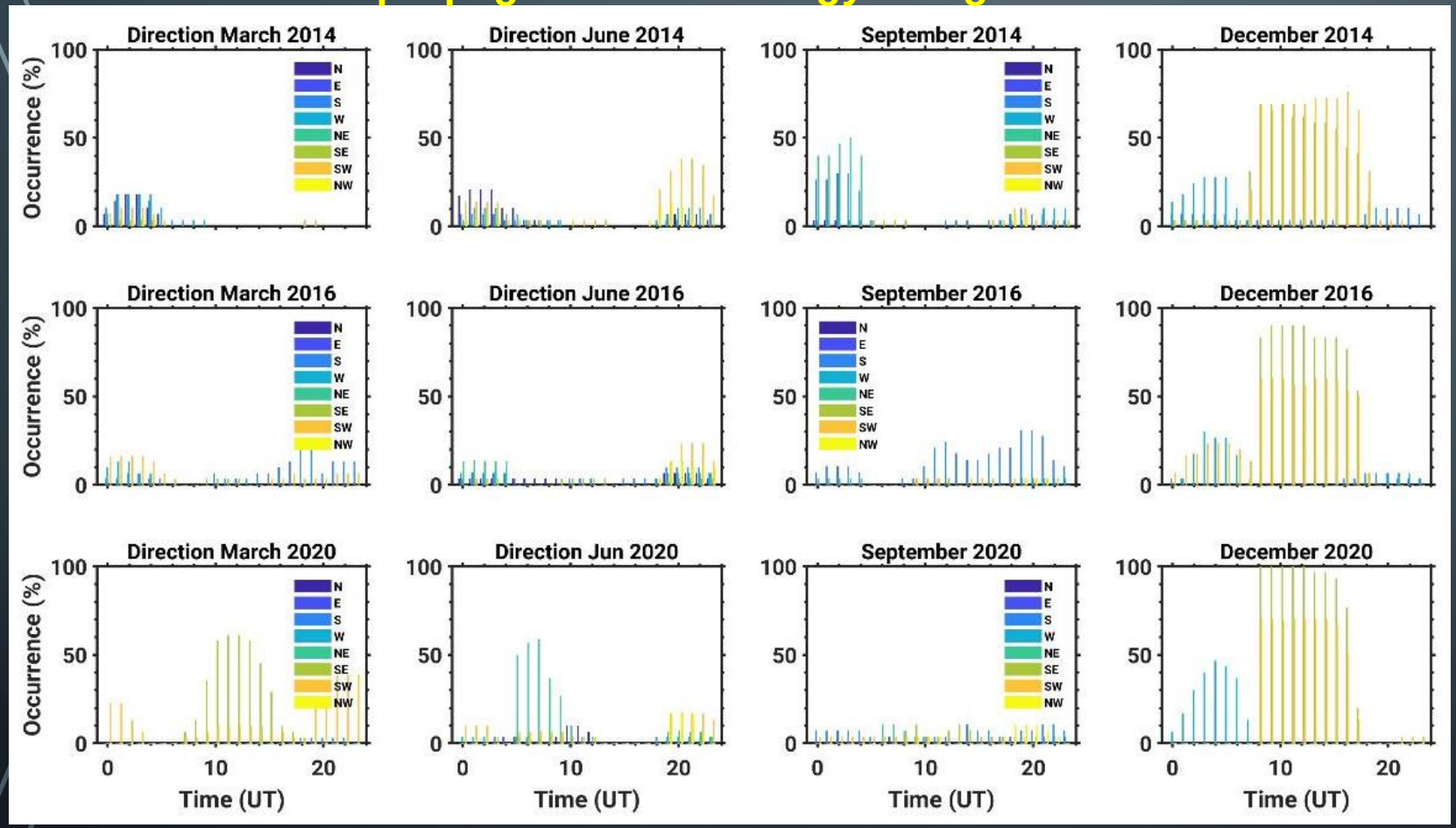

- Most often the daytime MSTID propagates towards southwest or southeast
- Pre-midnight MSTID propagates towards southwest
- Post-midnight MSTID propagates either southwest or northeast
- In 2020, significant number of northeast and westward propagating early morning MSTID are noted in June and December, respectively

RESULTS: MSTID CLIMATOLOGY

Solar activity dependency of MSTID occurrence using ionograms

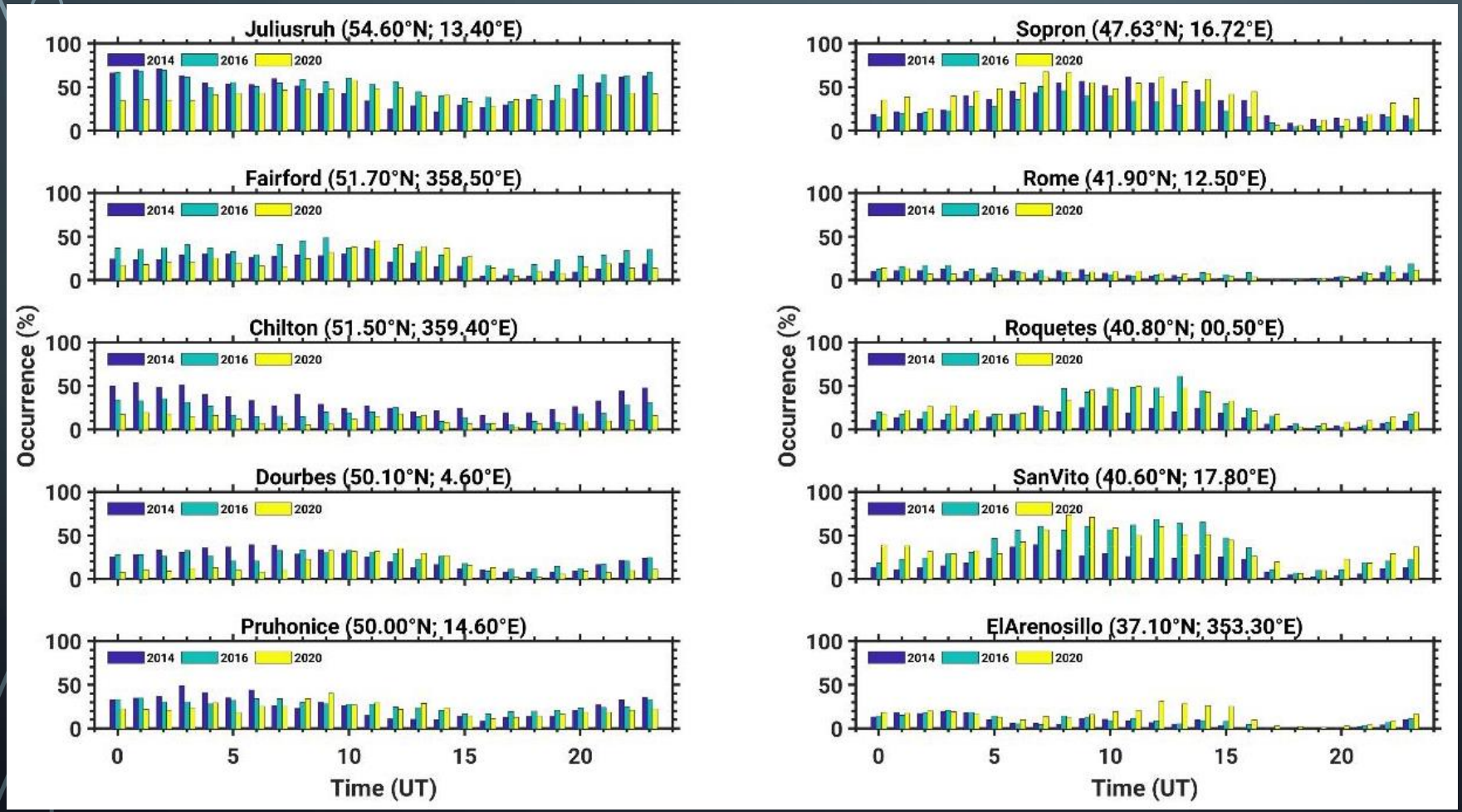

- ✓ Post-midnight TIDs occurrence is higher in solar maximum year than solar minimum years above 50°N and this pattern reverse below 50°N.
- ✓ Daytime and pre-midnight TIDs occurrences are more during the moderate and lower solar activity years below 50°N

RESULTS: COMPARISON

Comparison between dTEC and ionogram estimated MSTID occurrence characteristics

- ✓ In December solstice, both data sets show the negative solar activity dependency of the daytime MSTID occurrence, however there is a significant difference in the occurrence percentage, i.e. the occurrence rate is more than 90% in dTEC but it is always below 60% in all the ionosonde stations.
- ✓ From the dTEC data, the daytime MSTID occurrence is very small (less than 20%) during the equinox months (except March 2020), but the ionogram analysis indicates occurrence of daytime MSTID more than 40% in most of the stations.
- ✓ Post-midnight MSTID occurrence is more pronounced during the March equinox and it also indicates a positive solar activity dependency and this feature is also present in the ionograms. However, the ionosonde observations show two distinct behaviors based on the latitude as far as the solar activity concerns. In the high-mid latitudes pre-midnight MSTID occurrence shows a positive correlation with solar activity and in the mid latitudes it shows a negative solar cycle dependency.

MSTID CLIMATOLOGICAL MODEL

- Assumption 1: The prediction for the MSTID occurrence is assumed to rely exclusively on extreme dTEC values.
- Assumption 2: The dTEC value depends on the geographical location (GL), local time (LT), ap index and solar proxy (SP: F10.7 cm).
- Assumption 3: The dependence of dTEC from GL, LT, ap index and SP is linear.

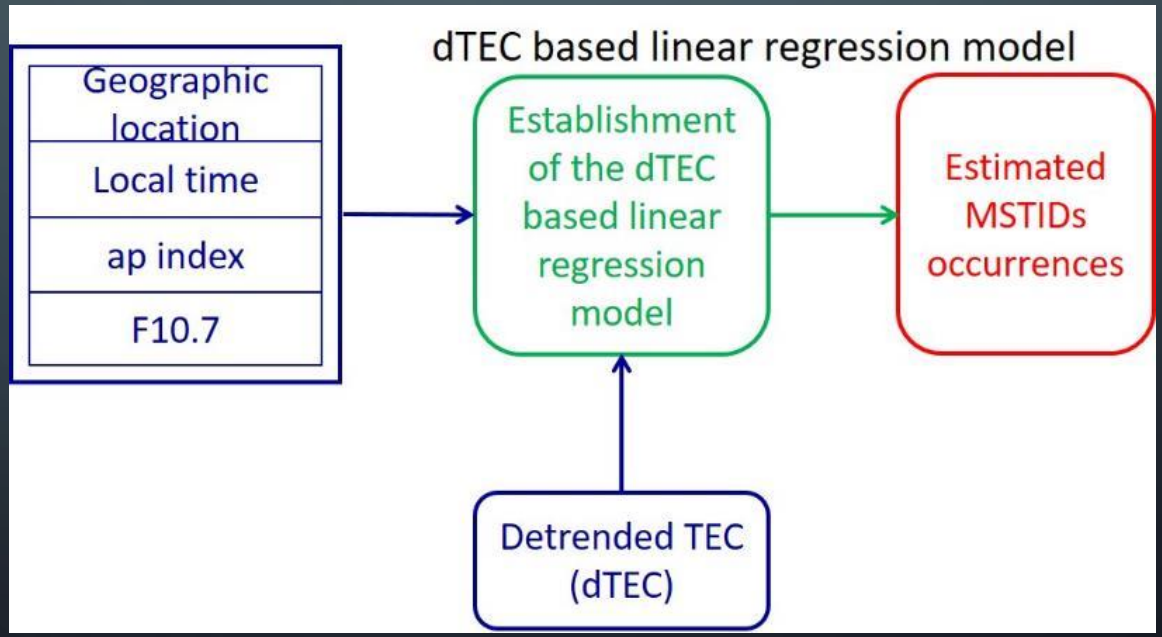

MSTID CLIMATOLOGICAL MODEL

To develop the model, we use the linear regression equation as follows

$$\mathrm{dT} = \alpha_0 + \alpha_1 \mathrm{ap} + \alpha_2 \mathrm{LT} + \alpha_3 \mathrm{SP} + \alpha_4 \mathrm{GL} \ldots\ldots. (1)$$

The estimation of the coefficients $\alpha_0, \ldots, \alpha_4$, relies on a set of n observations of the form

$\big((ap_i, LT_i, SP_i, GL_i), dTEC_i\big)$, $i = 1, \ldots, n$, so that the least square criterion

$J = \sum_{i=1}^{n} \big(dTEC_i - (a_0 + a_1 \cdot ap_i + a_2 \cdot LT_i + a_3 \cdot SP_i + a_4 \cdot GL_i)\big)^2$ is minimized.

Defining the $N \times 5$ matrix $X = \begin{bmatrix} 1 & ap_1 & LT_1 & SP_1 & GL_1 \\ 1 & ap_2 & LT_2 & SP_2 & GL_2 \\ \vdots & \vdots & \vdots & \vdots & \vdots \\ 1 & ap_n & LT_n & SP_n & GL_n \end{bmatrix}$,

the n-dim. column vector $\boldsymbol{y} = \begin{bmatrix} dTEC_1 \\ dTEC_2 \\ \vdots \\ dTEC_n \end{bmatrix}$ and the 5-dim. column parameter vector $\boldsymbol{a} = \begin{bmatrix} a_0 \\ a_1 \\ \vdots \\ a_4 \end{bmatrix}$,

it turns out (e.g., Theodoridis *et al*, 2009) that the least squares solution for $\boldsymbol{a}$ is

$$\hat{\boldsymbol{a}} = \begin{bmatrix} \hat{a}_0 \\ \hat{a}_1 \\ \vdots \\ \hat{a}_4 \end{bmatrix} = (X^T X)^{-1} X^T \boldsymbol{y}$$

where the superscript T is the transpose operator.

MSTID CLIMATOLOGICAL MODEL: PRELIMINARY RESULTS

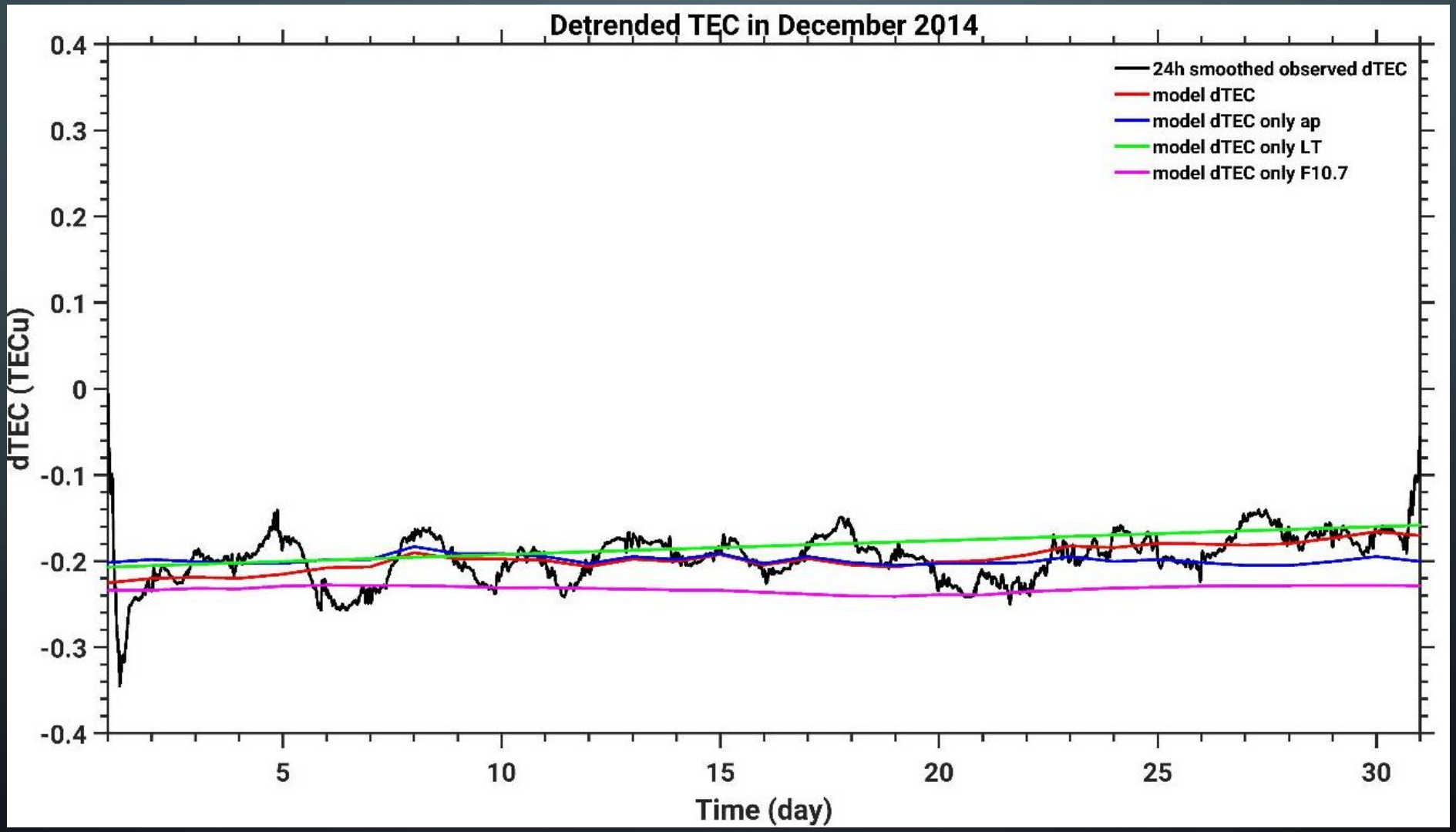

MSTID CLIMATOLOGICAL MODEL

From assumption 1, extreme values of $dTEC$ are those that are outside the interval $(-0.2, 0.2)$. The rule for the identification of an MSTID occurrence is to have for two to six successive time stamps either $dT > 0.2$ or $dT < -0.2$ (in more compact form $|dT| > 0.2$), considering the temporal resolution of the dT is 5 minutes ($|dT| > 0.2$ for more than six successive time stamps is indicative of LSTIDs). In order to define an index I that quantifies how likely is the MSTID to occur, we consider a past time window of size greater than 8. Then, I could be defined as follows: If the above defined rule is fulfilled for the dT values in the above interval, then $I = 1$. Otherwise, consider the maximum of all dT values, dT_{max}, that is less than 0.2 within the window and define the index as

$$I = \exp\left(-(0.2 - |dT_{max}|)\right)$$

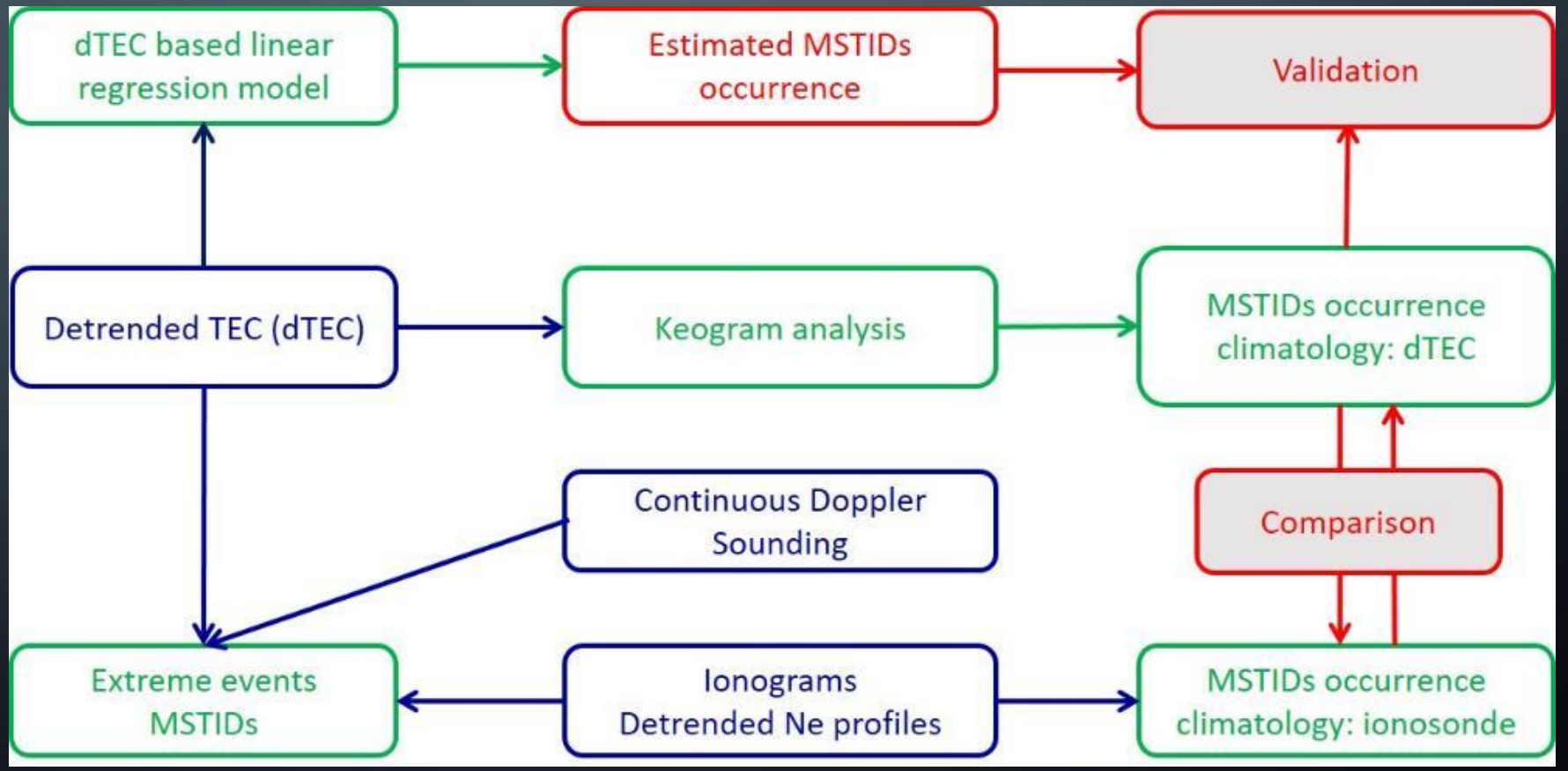

Summary

- ✓ GAIA model can successfully reproduce seasonal variation of the daytime MSTIDs.
- ✓ MICO model explains the role of Es layer instability and Perkins instability in the generation of nighttime MSTIDs. It also provide an information about the scale dependency of the E and F region coupling
- ✓ SAMI3 can reproduce the northwest to southeast aligned phase fronts but fails to reproduce the southwest propagation of the nighttime MSTIDs
- ✓ MSTIDs climatological model is under development.